

Differential Proteome of the Striatum from Hemiparkinsonian Rats Displays Vivid Structural Remodeling Processes

Grit Lessner,^{†,‡} Oliver Schmitt,^{*,†,‡} Stefan J.-P. Haas,[‡] Stefan Mikkat,[§] Michael Kreutzer,[§] Andreas Wree,[‡] and Michael O. Glocker[§]

Department of Anatomy, Gertrudenstrasse 9, 18055 Rostock, Germany, and Proteome Center Rostock, Schillingallee 69, 18055 Rostock, Germany

Received April 30, 2010

Parkinson's disease is a multifactorial, neurodegenerative disease where etiopathogenetic mechanisms are not fully understood. Animal models like the neurotoxic 6-OHDA-hemiparkinsonian rat model are used for standardized experiments. Here, we analyzed proteome changes of the striatum three months after 6-OHDA lesions of the nigral dopaminergic cell population. Striata were removed and proteins were separated by 2DE followed by differential spot analysis. Proteins in spots were identified by MALDI-TOF-MS. Most up-regulations of proteins were concerning energy metabolism in mitochondria. Proteins of calcium homeostasis like annexin A3, annexin A7, calbindin, calmodulin, calreticulin, and reticulo-calbin 1 also were differentially regulated. Moreover, proteins involved in antioxidative mechanisms like superoxide dismutase, protein disulfide isomerase 1 and 3, *N(G),N(G)*-dimethylarginine dimethylaminotransferase 2, and thioredoxin-dependent peroxide reductase were up-regulated. Interestingly, most cytoskeletal proteins belonging to the axon cytoskeleton and synapse were up-regulated pointing to long-distance axon remodeling. In addition, transcription factors, proteins of nucleic acid metabolism, chaperones, and degrading proteins (UCHL1) were up-regulated as well. In conclusion, the neurotoxin-induced proteome alterations indicate vivid long-distance remodeling processes of dendrites, axons, and synapses that are still ongoing even three months after perturbation, indicating a high plasticity and regeneration potential in the adult rat brain.

Keywords: Parkinson's disease • striatum • 6-OHDA • differential proteome analysis • MALDI-TOF-MS

Introduction

Idiopathic or sporadic Parkinson's disease (PD) is the most common neurodegenerative disorder after Alzheimer's disease with a prevalence of about 2% among people over 65 years. PD is a progressive disorder showing severe motor symptoms including tremor, bradykinesia, rigidity and postural instability.^{1–7} PD likely has multiple interacting causes that include increased oxidative stress damage to mitochondrial components and reduced mitochondrial bioenergetic capacity. The striatum is the first region that is affected functionally and chemically by the death of dopaminergic neurons in the substantia nigra (SN). However, the precise mechanisms and specific proteins responsible for mediating these effects remain to be elucidated.

Hence, the identification and biological evaluation of novel proteins involved in these pathways is critically providing a more comprehensive understanding of PD progression and protein interactions in animal models of PD. A reproducible loss of nigrostriatal dopaminergic neurons, similar to effects

observed in PD, is achieved by intracerebral administration of the neurotoxin 6-hydroxydopamine (6-OHDA), a hydroxylated analogue of the natural neurotransmitter dopamine (DA). 6-OHDA is selectively transported into dopaminergic neurons through dopamine transporters (DATs). Inside neurons, 6-OHDA accumulates in the cytosol and induces cell death without apoptotic characteristics (apoptosis).^{8,9} Therefore, unilateral stereotaxic injection of 6-OHDA in the medial forebrain bundle (MFB) is a common animal model of PD "the Hemiparkinsonian rat".^{10,11} The neurotoxin is retrogradely transported to the substantia nigra pars compacta (SNc) and destroys selectively dopaminergic neurons resulting in an ipsilateral dopaminergic denervation of the striatum within 12 h and striatal dopamine levels are depleted 2–3 days later.^{12–14} As in PD, this model results in a predominant reduction of dopamine levels in the dorsal striatum. Apomorphine is a dopamine receptor agonist that stimulates two classes of striatal dopamine receptors (D1, D2). The expression of contralateral turnings after systemic injections of apomorphine is generally considered to be a typical feature of unilateral 6-OHDA-lesions. However, at the moment, there is sparse information of the different metabolic pathways in the 6-OHDA-rat-model of PD available because most studies have been performed on MPTP-mice models or transgenic mice models.^{15,16} Recent findings indicate the impact of disease progress in terms of neuronal proteins of the

* To whom correspondence should be addressed. Prof. Dr. Oliver Schmitt, Department of Anatomy, Gertrudenstr. 9, 18055 Rostock, Germany. Phone: +49 0381 4948408. Fax: +49 0381 4948402. E-mail: schmitt@med.uni-rostock.de.

[†] These authors contributed equally to this work.

[‡] Department of Anatomy.

[§] Proteome Center Rostock.

cyto-, dendro- and axoskeleton. Among these structural proteins are actins and their interactions with α -synuclein^{17–19} and parkin¹⁸ as well as tubulins.²⁰ Thus, this study focuses on alterations of structural proteins of the neuronal compartment^{21–23} that are associated with remodeling of nerve fibers in the 6-OHDA model of PD. Hence, we wanted to know how the striatal proteome reacts on neurotoxic deafferentiation, as such changes could be comparable with those in the striatum of PD patients.

Two further aspects should be emphasized. First, the comparison of differential proteomics of the neurotoxic rat model with the striatum of Parkinsonian patients from other studies could shed light on the reproducibility of this basic animal model and the human patient.^{24–29} Second, if we detect and understand differences in the proteome of lesioned and control striata, these can be targets for more specific therapies and may support therapeutic neuronal progenitor cell transplantations.^{30–37}

The 6-OHDA lesion can be considered as the starting point for subsequent pharmacotherapy, transplantation and/or gene therapy experiments.³⁸ To detect differences of the proteome after experimental therapies it is necessary to understand changes of the proteome within different experimental steps. The first experimental step (control versus 6-OHDA lesioned striatum) has been analyzed in this region-specific³⁹ neuroproteomic study.

In the present study, we determined whether protein expression would be altered in the striatum of rats following 6-OHDA-induced dopaminergic denervation of the rat striatum by destroying neurons from the substantia nigra. To achieve this we used a 2DE-based proteomics approach in combination with sophisticated image analysis software, matrix assisted laser desorption/ionization time-of-flight (MALDI-TOF) mass spectrometry (MS) and peptide mass fingerprinting (PMF) and pathway analysis (Kyoto Encyclopedia of Genes and Genomes KEGG (version KEGG2, 20.02.2009, <http://www.genome.ad.jp/kegg/>),^{40–42} Reactome, ConsensusDB, Pathway Architect (v2.0.1, Agilent, Stratagene)).

Experimental Section

Six weeks old male Wistar rats (Charles River, Sulzfeld) were initially used in the control and in the experimental group (6-OHDA lesion) to reduce sex and age variation of protein expression levels. The animals weighed between 280–310 g at the beginning of the experiment. They were housed at 22 °C \pm 2 °C under a 12 h light-dark cycle with free access to food and water. All animal treatment and experimental procedures were conducted in compliance with the regulations and licensing of the local authorities (Landesamt für Landwirtschaft, Lebensmittelsicherheit und Fischerei Mecklenburg Vorpommern, Germany) and Animal Care and Use Committee of the University of Rostock. According to the European Communities Council Directive of 24 November 1986 (86/609/EEC) and in accordance with the above-mentioned local authorities adequate measures were taken to minimize pain or discomfort.

6-OHDA Lesion Surgery. 34 Wistar rats were lesioned to allow selection only of those 6 animals that were reaching a threshold in behavioral testing indicating a successful lesioning. The substantia nigra of these rats—deeply anesthetized with pentobarbital-Na⁺ (45 mg/kg BW ip)—were unilaterally lesioned by an injection of 6-OHDA-HCl (6.5 μ g/ μ L in 0.02% ascorbic-saline, Sigma-Aldrich) into the right medial forebrain bundle (26 μ g/4 μ L/4 min) at the following coordinates (in mm relative

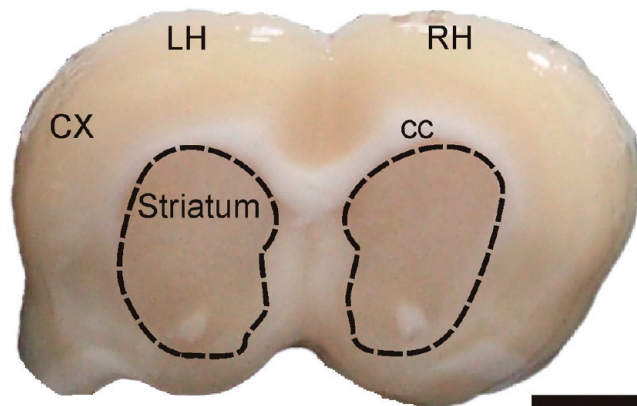


Figure 1. Perfused and dissected brain with left hemisphere (LH), right hemisphere (RH), cortex (CX) and the corpus callosum (cc). The dashed lines are marking the regions of the striatum that were used for proteome analysis. Scale bar: 2.5 mm.

to bregma and the interaural axis: anterior-posterior axis -2.3 , mediolateral axis -1.5 , ventral axis 1.5).⁴³ Injections were performed using a 5 μ L Hamilton microsyringe with a 26-gauge steel cannula (Hamilton, Bonaduz, Switzerland).

Apomorphine-Induced Rotations and Statistics. We used the nonselective D1-, D2-receptor agonist apomorphine, which causes contralateral rotations in hemilesioned animals, as a way to determine completeness of the 6-OHDA-lesions, since it is difficult to determine completeness of a striatal dopaminergic deafferentiation by amphetamine.^{44–50} To assess the efficacy of the lesions, all rats were tested for apomorphine-induced rotations.^{51,52} Apomorphine (0.25 mg/kg BW) (Teclapharm), dissolved in saline, was injected s.c. Three months after lesion and induced rotations were monitored over 40 min using an automated rotometer system according to Ungerstedt and Arbuthnott.⁵¹ Only the rats showing rotational scores >4 net full turns/minute in the direction contralateral to the lesion were selected for the study, corresponding to $>97\%$ depletion of DA tissue levels^{53,54} in the striatum on the side ipsilateral to the lesion. As an internal control the rotations of nonlesioned animals ($n = 6$) were also tested (0.15 rot/min \pm 0.32). Those differences with a $p \leq 0.05$ in the U-test are considered to be significant. Tests were performed with SPSS 11.01 (SPSS Inc.).

Perfusion and Dissection. 6-OHDA lesioned animals ($n = 6$, 134 days of age¹⁴) and control animals ($n = 6$, 122 days of age) were killed with an i.p. pentobarbital-Na⁺ injection of 60 mg/kg BW). Transcardial perfusion was performed with 0.9% NaCl. After brain dissection the striatum (Figure 1) was removed using a brain matrix (WPI, Sarasota, USA) and a 5 mm punch (WPI, Sarasota, FL) (Figure 1). The fresh material was put into cooled Eppendorf-tubes, weighed and stored at -80 °C until homogenization. From pentobarbital injection to -80 °C storage it took less than 5 min. The efficacy of the 6-OHDA lesion was confirmed post mortem, by tyrosine hydroxylase immunohistochemistry (Figure 5).

Homogenization. Protein extraction was performed according to published standardized protocols^{55–57} with specific adaptations described in the following. The striatum tissue was incubated with (9 \times probe mass [mg]) μ L sample buffer consisting of 7 M urea (Sigma, Steinheim, Germany), 2 M thiourea (Sigma), 4% CHAPS (Sigma), 70 mM DTT (Sigma), 0.5% Bio-Lyte Ampholytes pH 3–10 (Fluka, Buchs, Switzerland) and a mixture of protease inhibitors (Roche, Basel Switzerland) additionally enriched with (0.1 \times probe mass [mg]) μ L Pepstatin

2DE of 6-OHDA Lesioned Striatum

A (Sigma) and PMSF (Fluka) and shock frozen at -180°C . The samples were quickly thawed and transferred into a 2 mL Wheaton potter (neo-lab, Heidelberg, Germany) for homogenization. Glass beads (Roth, Karlsruhe, Germany) were added to the suspension, following a 15 s sonication, 15 s vortexing, 1 min swinging cycle which was repeated six times and finished by shock freezing the suspension at -180°C . The samples were quickly thawed. They were put in a beaker on a magnetic stirrer that was filled with ice–water for 15 min. Finally the samples were centrifuged at $17\,860\times g$ for 20 min at 4°C (Megafuge Kendro, Osterode, Germany). The supernatant was very carefully removed using a 2 mL syringe (Becton Dickinson, Heidelberg, Germany) with a 0.5×25 mm needle (Becton Dickinson), because of a thick lipid coverage derived from myelinated nerve fibers. The protein content of the supernatant was determined by the Bradford assay.⁵⁸

2DE. 2DE was performed as described.^{55,56} Briefly, the first dimension was carried out in a PROTEAN IEF cell system (Bio-Rad, Munich, Germany). Protein extracts of 1 mg protein were loaded on immobilized pH 3–10 nonlinear gradient strips with a length of 17 cm (Bio-Rad) and actively rehydrated with 300 μL rehydration buffer consisting of 6 M urea (Sigma), 2 M thiourea (Sigma), 2% CHAPS (Sigma), 16 mM DTT (Sigma), 0.5% Bio-Lyte Ampholytes pH 3–10 (Fluka) at 50 V for 12 h at 20°C . After rehydration electrode wicks (Bio-Rad) were added to reduce artifacts. Focusing started with a 1 h linear increase to 250 V, followed by a 3 h gradual increase to the final voltage of 8000 V and kept constant until a total of 99 999 Vhrs (after approximately 12.5 h) were reached. During the whole IEF the temperature was constantly hold at 20°C .^{59,60} After focusing the strips were stored at -80°C .

Focused IPG strips were equilibrated in two consecutive steps of 30 min each in 5 mL of freshly prepared SDS equilibration solution consisting of 1.5 M Tris-HCl pH 8.8 (Roth), 6 M urea (Sigma), 30% Glycerol (Sigma), 2% SDS (Sigma), trace of bromophenol blue (Roth) supplemented with 10 mg/mL DTT and 40 mg/mL iodoacetamide, respectively. The strips were transferred on 12% homogeneous self-cast sodium dodecyl sulfate polyacrylamide gels (200 mm \times 250 mm \times 1.5 mm). They were run at 125 V per gel (Power Pac 1000, Bio-Rad) in the PROTEAN Plus Dodeca Cell (Bio-Rad). A cooling device (Julabo F10, Julabo Labortechnik, Seelbach, Germany) was used to ensure a constant buffer-temperature of 10°C . Each run was done with those 12 strips that would be analyzed differentially.

Protein Visualization and Image Analysis. The gels were fixed in 45% methanol and 1% acetic acid for 6 h and then stained in a solution of colloidal Coomassie brilliant blue G250 (1 g/1000 mL) (Roth) for 24 h as previously described.^{61,62} The stained gels were scanned as 16 bit gray scale tif-images with a F4100 scanner (Heidelberg, Heidelberg, Germany) at 300 dpi resolution. Gels were rinsed in 0.02% sodium azide (Aldrich-Chemie, Steinheim, Germany), shrink-wrapped in plastic and stored at 4°C until picking for MALDI-TOF-MS.

For 2DE gel image analysis, the software package Progenesis PG200 Version 2006 (Nonlinear Dynamics Ltd., Newcastle upon Tyne, U.K.) was used. Gels were registered to a reference gel (gel showing most spots with highest separation and staining quality and least artifacts) and edited spots were matched to allow comparability of all gels. Protein spots in 2DE were quantified by normalizing spot volumes using the Progenesis PG200 and spot volume differences were calculated.⁶³ Only those spots were considered to be significantly up- or down-

regulated that showed a 2-fold larger or lower spot volume in at least 3 different gels. The filtered spots were picked automatically using the Flexys Proteomics picker (Genomic Solutions, Ann Arbor, MI) with a 1 mm² picking tool.

In-Gel Enzymatic Digestion of Proteins. Excised protein spots were subjected to in-gel digestion with trypsin.⁶⁴ Briefly, gel plugs were washed twice with 30% acetonitrile (ACN) in 25 mM ammonium bicarbonate and 50% ACN in 10 mM ammonium bicarbonate, respectively, shrunk with ACN, and dried at 37°C . The dried gel plugs were reswollen with 5 μL protease solution (sequencing grade trypsin, 10 ng/ μL in 3 mM Tris-HCl, pH 8.5, Promega, Madison, WI and incubated for 5–8 h at 37°C . Thereafter, 5 μL of extraction solution (0.3% TFA, 50% ACN) were added and the samples were agitated at room temperature for 30–60 min.

MALDI-TOF-MS Analysis and Database Search. The resulting peptide-containing solution was prepared onto the MALDI target (384/600 μm AnchorChipTM, Bruker Daltonik, Bremen, Germany) according to⁶⁵ with slight modifications. The peptide sample (0.8 μL) was applied onto the sample anchor and allowed to evaporate for a few minutes. Prior to drying, 1.8 μL CHCA solution (1.6 mM CHCA in ethanol/acetone 67/33 [v/v]) were added and allowed to dry at room temperature. The sample was washed with 5 μL of 1% TFA that were removed after 30 s by means of filter paper. Peptide mixtures were analyzed by MALDI-TOF-MS using a Reflex III mass spectrometer (Bruker Daltonik) equipped with the SCOUT source, delayed extraction, and operated in positive ion reflector mode with an acceleration voltage of 20 kV.⁶⁶ Mass spectra were acquired and analyzed automatically using Bruker software, but, if necessary, peak picking and calibration were corrected manually using FlexAnalysis 2.4 (Bruker Daltonik). For internal calibration three peptides arising from trypsin autolysis (m/z 842.51, m/z 2211.10, and m/z 2807.35) were used. Background peaks were removed applying a list containing mainly products from trypsin autolysis. Proteins were identified by searching a regularly updated in-house SWALL sequence database (Swiss-Prot and TrEMBL, release 2010_06 containing 113686 rodent sequences and 31 644 sequences from Rattus) using the MASCOT 2.2 software (Matrix Science, London, U.K.) via BioTools 3.0 software (Bruker Daltonik). A mass tolerance of 60 ppm and 1 missing cleavage site were allowed, oxidation of methionine residues was considered as variable modification, and carbamidomethylation of cysteines as fixed modification.^{67,68} The search was first restricted to proteins from Rattus and thereafter repeated for rodent proteins to include proteins still missing in the sequence data of Rattus. All results were examined carefully for reliability and occurrence of multiple proteins in the same sample. If the database search against the SWALL sequence database resulted in homologous proteins to which the same number of matched peptides were assigned, the entry from Swiss-Prot, if existing, was selected. Entries from TrEMBL were used only, if no homologous protein was contained in Swiss-Prot or if a higher number of peptides matched to a sequence from the TrEMBL database.

Immunohistochemical Procedures. Preparation of the animals for immunohistochemistry and histology were performed after proteome analysis. After anesthesia with pentobarbital (see above), the rats were perfused transcardially with ice cold 0.9% sodium chloride (50 mL), followed by 400 mL of 3.7% paraformaldehyde (dissolved in 0.1 M PBS, pH 7.4). Brains were immediately removed from the skull, postfixed for 4 h, and

transferred into PBS (pH 7.4) containing 20% sucrose overnight at 4 °C. The cryoprotected brains were frozen in isopentane (−50 °C) and stored at −80 °C until further processing. Thirty micrometer thick cryostat sections were, after two rinses in 0.1 M PBS, incubated for 20 min in 3% H₂O₂ to quench endogenous peroxidases. Sections were then rinsed three times in 0.1 M PBS and incubated for one hour in 0.1 M PBS containing 0.025% Triton X-100 (Sigma), 3% BSA and 3% normal horse serum (Vector Laboratories), followed by an incubation over 48 h at 4 °C with the primary antibodies against TH (mouse monoclonal, clone TH-2, 1: 1000, Sigma), dissolved in 0.1 M PBS containing 0.05% Triton X-100 and 1% BSA. After three washes in 0.1 M PBS sections were incubated overnight at 4 °C with biotinylated secondary antibodies directed against mouse IgG (horse polyclonal, 1:200, Vector Laboratories) followed by three washes in 0.1 M PBS, then for 2 h in the ABC-complex (1: 50 for solutions A and B, Vector Laboratories), and after three rinses in 0.1 M PBS the final detection with 0.02% DAB (Sigma) for 8 min at room temperature was performed. Sections were mounted onto gelatin coated glass slides, dehydrated in graded alcohol concentrations and coverslipped with DePeX mounting medium (Serva).

Results

The successful lesioning of dopaminergic neurons in the substantia nigra (cf. Figure 5) was controlled by applying the rotation measurement after s.c. injection of apomorphine and was found to stand in agreement with published data.^{48,50,51} Animals exhibiting more than 4 rotations per minute and matching controls were selected for proteome analysis. The mean rotation per minute of the 6 lesioned animals was 7.25 ± 0.44 SEM.

To identify specific differences in protein expression among the control and lesion group, we used 2D-gel electrophoresis with subsequent gel-matching, spot-warping and spot difference analysis combined with protein identification by MALDI-TOF-MS. Spot localization was performed automatically followed by an extensive interactive verification. Differential expression of spots was determined by calculating the quotients of spot volumes. If quotients were ≥2 or ≤0.5 in more than 2 gel pairs then we classified them as up- respectively down-regulated. Some proteins were detected in more than one spot. Moreover, some proteins were identified in spots containing also other proteins (23 mixed spots). These findings are explicitly presented in Supplement Table 1 and Supplement Figure 3 (Supporting Information). On average 1374 spots were detected in the 6 gels of the control group and 1274 spots in the 6 gels of the lesion group. In order to check for reproducibility of spot abundant differences, each group was analyzed separately. 56 spots were found to be present in all 6 gels, 39 spots were matched in 5 gels, 26 spots were matched in 4 gels and 23 spots in 3 gels. Hence, most of the spots could be successfully matched in more than 3 gels.

Next, an overview of quantitative spot abundance differences analyzed by comparing the 6 gels from 6 control animals with the 6 gels from 6 successfully lesioned animals is given. In the supplement the specific up- and down-regulations of specific proteins are interpreted in a functional way with regard to network interactions and pathways. By comparing the control and the lesioned group (Figure 2) 144 spots were found to be differentially expressed. A total of 101 proteins in these 144 differentially expressed spots were identified (supplement Figure 1) using MALDI-TOF-MS (Table 1). Twenty-nine of the

101 identified proteins were down-regulated, 70 proteins up-regulated. One spot (PURA) was absent in the control group.

The differentially expressed proteins were grouped into 9 functional protein groups (Supplemental Figure 1, Supporting Information) whereas the enzyme group was further subdivided comparable with a classification for protein mapping in neuronal systems.³⁹ The enzyme group contains 46% or a total of 46 of all differentially regulated proteins. Structural proteins like cytoskeleton proteins are the second largest group with a total of 20 (20%) proteins. We found 9 (9%) regulating proteins, 4 (4%) transport proteins and 7 (7%) proteins involved in protein folding (chaperones) that all were differentially expressed as was determined by differential gel analysis. Only 1 protein (1%) of the differentially expressed proteins was found to belong to cell cycle proteins. Five (5%) transcriptional proteins and 8 (8%) that were assigned to signal transduction were differentially regulated. In the group of enzymes, 9 (9%) belong to energy metabolism and 8 (8%) to carbohydrate metabolism. Nine (9%) enzymes are involved in amino acid, 4 (4%) in nucleic acid and 4 (4%) in lipid acid metabolism. Importantly, 6 (6%) enzymes of the antioxidant group were identified. We found 3 (3%) proteins that are cofactors and involved in the metabolism of vitamins, 2 (2%) enzymes that belong to the proteasome degradation system and one enzyme (tyrosine hydroxylase, TH) that is involved in dopamine synthesis. It should be noted that in protein lysates from the 6-OHDA lesioned striatum, TH was extremely down-regulated (Figure 3), which was validated by immunohistochemistry (Figure 5). The lesioned striatum shows a strong reduction of TH immunoreactivity. The nigrostriatal denervation can be visualized using immunohistochemical demonstration of tyrosine hydroxylase (TH) the rate limiting enzyme of the synthesis of DA. TH is transported from the SNC to the striatum anterogradely.

In the following the differential regulations of the members of 9 protein groups (Supplemental Figure 1, Supporting Information) and their enzyme-subgroups (9) as well as their network interactions are described (Table 1). Their specific functions, appearance in the CNS (Supplemental Figure 2, Supporting Information) and involvement in diseases are put into relation to PD and the 6-OHDA model of PD in the supplement. In several spots more than one protein was identified by MALDI-TOF-MS analysis. These protein mixes are documented in detail in Suppl. Tab. 1, and annotated in the reference gel (Supplemental Figure 3, Supporting Information). Furthermore, the number of matches of spots in gels of the lesioned animals and the extent of up- and down-regulation are documented in Supplemental Table 2 (Supporting Information).

With regard to proteome analysis we are investigating a *long-distance* effect of the striatal proteome that reacts *indirectly* following the retrograde 6-OHDA lesion of the SN dopaminergic neuron population. Hence, problems of data interpretation due to inflammation processes (cf. refs 69, 70) of the investigated structure do not affect the striatal proteome.

The up- and down-regulated structural proteins belong to astrocytes (vimentin), the axonal cytoskeleton (tubulin beta, internexin, neurofilament) and herein proteins involved in actin processing as well as synaptic (Septins, synapsin, clathrin cf. Table 1 and Supplemental Figure 2, Supporting Information) and dendritic proteins (drebrin). Dihydropyrimidinase related protein 2 (DPYL2) was found to be up-regulated in gels of lesioned animals. It acts on microtubule reorganization and

Table 1. Significantly Altered Protein Abundances of the Striatum of 6-OHDA Lesioned Rats^a

gene symbol		lesioned striatum	M _w (Da)	pI
Group 1		Structural proteins		
ACTB	Actin, cytoplasmic 1	DOWN	42052	5.29
ARP3	Actin related protein 3	UP	47783	5.61
INA	Alpha Internexin	UP	56253	5.2
DBNL	Drebrin-like protein	DOWN	48925	4.89
DPYSL2	Dihydropyrimidinase related protein 2	UP	62638	5.95
DPYSL4	Dihydropyrimidinase related protein 4	UP	61617	6.3
DPYSL5	Dihydropyrimidinase related protein 5	UP	62071	6.6
FSCN1	Fascin Fragment	UP	22110	5.86
NEFL	Neurofilament light polypeptide	DOWN	61355	4.63
SEPT8	Sept8 protein	UP	51562	5.74
SEPT6	Sept6 protein	UP	49219	6.36
STOML2	Stomatin like protein 2	DOWN	38504	8.74
TBA1A	Tubulin alpha 1A-chain	DOWN	50788	4.94
TBA4A	Tubulin alpha 4A-chain	UP	50634	4.95
TBB2A	Tubulin beta 2A chain	UP	50274	4.78
TBB2C	Tubulin beta 2C chain	UP	50225	4.79
TBB3	Tubulin beta 3 chain	UP	50842	4.82
TBB5	Tubulin beta 5 chain	DOWN	50095	4.78
VIM	Vimentin	UP	53757	5.06
Group 2		Regulating proteins		
ANXA3	Annexin A3	UP	36569	5.96
ANXA7	Putative uncharacterized protein Anxa7	UP	50272	5.91
CALM1	Calmodulin 1	DOWN	16827	4.09
LASP1	Lim and SH3 domain protein 1	UP	30351	6.61
BIN1	Myc box dep.-interacting protein 1	DOWN	64721	4.95
RCN1	Reticulocalbin 1	DOWN	38090	4.7
STIP1	Stress induced phosphoprotein 1	UP	63158	6.4
SYN2	Synapsin 2	UP	63702	8.73
WDR1	WD repeat containing protein 1	UP	66824	6.15
Group 3		Transport proteins		
NECAP1	Adaptin ear-binding coat-associated protein 1	UP	29831	5.97
CLTA	Clathrin light chain A	UP	27078	4.41
PITPNA	Phosphatidylinositol transfer protein α -isoform	UP	32115	5.97
VDAC1	Voltage dep. anion selective channel protein 1	UP	30851	8.62
Group 4		Chaperones		
HSPD1	60 kDa heat shock protein, mitochondrial	UP	61088	5.91
CALR	Calreticulin	DOWN	48137	4.33
CCT6A	Chaperonin containing Tcp1, subunit 6A (Zeta 1)	UP	58437	6.63
HSPA8	Heat shock cognate 71 kDa protein	DOWN	71055	5.37
HSP90AA1	Heat Shock protein HSP 90 alpha	UP	85161	4.93
HSPA9	Stress 70 protein	UP	74097	5.97
CCT2	T-complex protein 1 subunit beta	UP	57764	6.01
Group 5		Cell cycle		
GMFB	Glial maturation factor beta	UP	16897	5.32
Group 6		Energy metabolism		
ATP5A1	ATP synthase subunit alpha, mt	DOWN	59831	9.22
ATP5B	ATP synthase subunit beta, mt	UP	56318	5.19
ATP5D	ATP synthase subunit delta, mt	UP	18809	6.17
UQCRC1	Cytochrom b-c1 complex subunit 1, mt	UP	53500	5.57
NDUFV2	NADH dehydrogenase [ubiquinone] flavoprotein 2, mt	UP	27703	6.23
NDUFA10	NADH dehydrogenase 1 alpha subcomplex subunit 10, mt	UP	40753	7.64
NDUFS8	Ndufs8 protein (NADH dehydrogenase (ubiquinone) Fe-S protein 8 predicted)	UP	24411	5.87
SDHA	Succinate dehydrogenase [ubiquinone] flavoprotein subunit, mt	UP	72596	6.75
ATP6VB2	Vacuolar ATP synthase subunit B, brain isoform	UP	56857	5.57
Group 7		Carbohydrate metabolism		
ACO2	Aconitase, mt	UP	86121	7.87
ALDOC	Fructose-bisphosphate aldolase C	UP	39658	6.67
ENO2	Gamma enolase	DOWN	47510	5.03
IDH3B	Isocitrat dehydrogenase subunit beta, mt	UP	42612	8.89
LDHB	L-lactat dehydrogenase B chain	UP	36874	5.7
MDH2	Malat dehydrogenase, mt	DOWN	36117	8.93
PDHA1	Pyruvat dehydrogenase E1 component subunit alpha, somatic form, mt	DOWN	43883	8.49
PKM2	Pyruvat kinase isoenzyme M1/M2	UP	58294	6.63
Group 8		Amino acid metabolism		
ASPA	Aspartoacylase-2	UP	35747	5.95
GOT1	Aspartate aminotransferase, cytoplasmic	UP	46628	6.73
CKB	Creatin kinase, B-typ	UP	42983	5.39
ALDH4A1	Delta-1-pyrroline-5-carboxylate dehydrogenase, mt	DOWN	62286	7.14
DLD	Dihydrolipoyl dehydrogenase, mt	UP	54574	7.96
GLUD1	Glutamate dehydrogenase 1, mt	UP	61719	8.05
GLUL	Glutamine synthetase	DOWN	42982	6.64
SIRT2	NAD-dep. deacetylase sirtuin-2	DOWN	39921	6.67
ALDH5A1	Succinate-semialdehyde dehydrogenase, mt	UP	56723	8.35
Group 9		Cofactors and vitamins		
BLVRB	Flavin reductase	UP	22297	6.49
PDXK	Pyridoxal kinase	DOWN	35114	6.32
PNPO	Pyridoxine-5'-phosphate oxidase	DOWN	30507	8.66

Table 1. Continued

gene symbol		lesioned striatum	M_w (Da)	pI
Group 10 Lipid metabolism				
ALDH2	Aldehyde dehydrogenase 2, mt	UP	56966	6.63
ACOT7	Cytosolic acyl coenzym A thioester hydrolase	UP	43164	8.8
GPD1L	Glycerol-3-phosphate dehydrogenase 1 like protein	UP	38828	6.34
PPT1	Palmitoyl-protein thioesterase 1	DOWN	34946	7.1
Group 11 Nucleic acid metabolism				
AK1	Adenylate kinase isoenzyme 1	UP	21684	7.66
ATIC	Bifunctional purine biosynthesis protein PURH	UP	64681	6.69
GDA	Guanine deaminase	UP	51554	5.56
ITPA	Inosine triphosphatase	UP	22255	5,48
Group 12 Antioxidants				
GSTM1	Glutathion-S-transferase Mu1	DOWN	26068	8.27
DDAH2	N(G),N(G)-Dimethylarginin, dimethylaminotransferase 2	UP	30011	5.66
P4HB	Protein disulfid isomerase	UP	57315	4.82
PDIA3	Protein disulfid isomerase 3	UP	57044	5.88
SOD2	Superoxide dismutase, mt	UP	24887	8.96
PRDX3	Thioredoxin-dep. peroxide reductase, mt	UP	28563	7.14
Group 13 Dopamine metabolism				
TH	Tyrosine-3-monoxygenase	DOWN	56330	5.74
Group 14 Proteasome				
FBXO2	Neural F box protein NFB42	UP	34021	4.3
UCHL1	Ubiquitine carboxyl terminal hydrolase L1	UP	25165	5.14
Group 15 Signal transduction				
YWHAE	14-3-3 Protein epsilon	DOWN	29326	4.63
YWHAG	14-3-3 protein gamma	DOWN	28456	4.8
YWHAZ	14-3-3 protein zeta/delta	UP	27925	4.73
MAPK2	Dual specificity mitogen activated protein kinase kinase 1	UP	43779	6.18
GNB1	Guanine nucleotide-binding protein G(I)/G(S)/G(T) subunit beta-1 (GTPase activity)	DOWN	38151	5.6
GNB2	Guanine nucleotide-binding protein subunit beta-2 (GTPase activity)	UP	38048	5.6
GNB5	Guanine nucleotide-binding protein subunit beta-5 (GTPase activity)	DOWN	39505	5.67
MAPK1	Mitogen activated protein kinase 1	UP	41648	6.5
Group 16 Transcription				
HNRNPA3	Heterogeneous nuclear ribonucleoprotein A3	DOWN	39856	9.1
HNRNPA32B1	Heterogeneous nuclear ribonucleoproteins B0a (Isoform A2/B1)	DOWN	32572	8.74
NAP1L4	Nucleosome assembly protein 1-like 4	UP	44118	4.58
RUVBL1	RuvB like 1	UP	50524	6.02
PURA	Transcriptional activator protein Pur-alpha	absent in controls	34976	6.07
Group 17 Unknown function				
C21ORF53	ES1 protein homologue, mt	UP	28497	9.11

“Proteins are classified and alphabetically sorted. UP, up-regulated; DOWN, down-regulated; M_w and pI , theoretical molecular weight and isoelectric point from Mascot report.

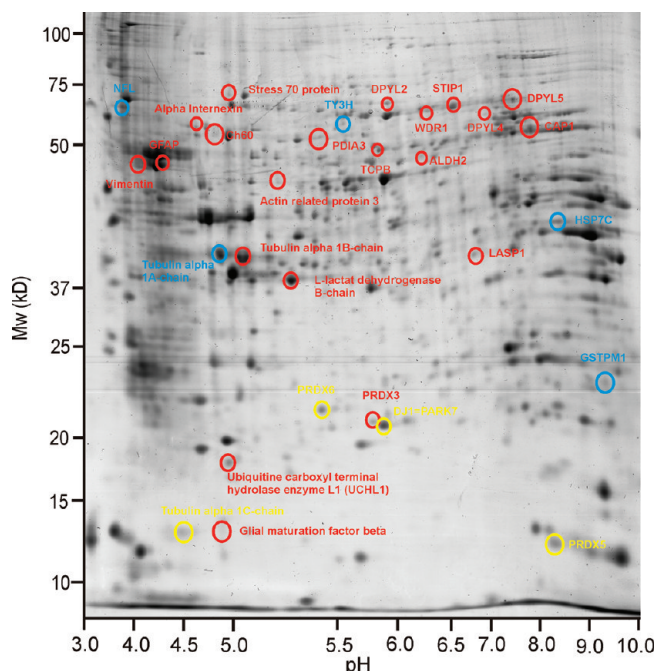


Figure 2. Typical gel of a lesioned animal showing differentially expressed spots. Red, up-regulated. Blue, down-regulated. Yellow, not differentially regulated.

consequently on axon repulsion. DPYL2 is also a component of the process of axon guidance and necessary during development. Dihydropyrimidinase related protein 4 (DPYL4) and Dihydropyrimidinase related protein 5 (DPYL5) have comparable functions as DPYL2 and are also up-regulated supporting the axon repulsion effect induced by 6-OHDA lesions. These observations are new and have not been described with regard to PD or PD models. The DPYL* elevation correlates with up-regulation of axonal proteins tubulin beta, alpha internexin and dynactin and all synaptic proteins that were identified (see Tab. 1 and Supplemental Figure 2, Supporting Information). In contrast, the dendritic protein drebrin-like was down-regulated.

In the group of regulating proteins, 6 proteins are up- and 3 are down-regulated. The up-regulation of several proteins used for actin processing is supported by an up-regulation of LIM and SH3 domain protein 1 (LASP1) in the lesioned striatum. Several regulating proteins associated with calcium homeostasis and signal transduction like the annexins A3 and A7 are regarded as up-regulated. Myc box-dependent-interacting protein 1 (BIN1) is regarded as down-regulated in the lesioned striatum.⁷² It is involved in regulation of synaptic vesicle endocytosis. Calmodulin (CALM), calreticulin (CALR) and reticulocalbin 1 (RCN1) are down-regulated. RCN1 is implicated in nerve regeneration⁷³ and located in neurons, astrocytes and Schwann cells.⁷⁴

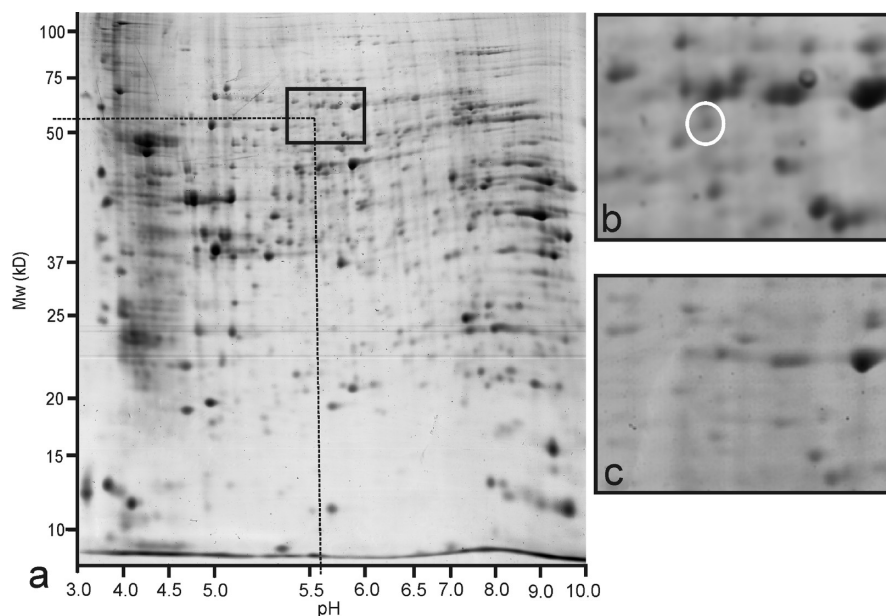


Figure 3. (a) Overview of a control gel with a rectangle around a region of spots containing the TH spot. The theoretical M_w of 56330 Da and the theoretical pI of 5.74 is indicated by dashed lines. (b) Magnification of the marked region in (a). The identified TH spot is marked by a circle. (c) TH spot is invisible in the regions of interest of gels derived from lesioned striata.

The up-regulated stress-induced-phosphoprotein 1 (STIP1) acts as a cochaperone. More importantly, STIP1 plays a role in cells to survive in stressful conditions,⁷⁵ for example, the 6-OHDA deafferentiation of the striatum. Furthermore, it is located specifically in post synaptic densities⁷⁶ and seems to be involved in synaptic plasticity.⁷⁷ In line with the up-regulation of STIP, synapsin II (SYN2) is up-regulated. A MALDI-TOF mass spectrum of SYN2 is presented in Figure 4. Synapsins associate as endogenous substrates to the surface of synaptic vesicles and act as key modulators in neurotransmitter release across the presynaptic membrane of axonal neurons in the nervous system. Recently, synapsin 2 was found to be dysregulated in PD and controls.⁷⁸ Along with these synaptic proteins, the up-regulated adaptin ear-binding coat-associated protein 1 (NECP1) and up-regulation of clathrin light chain A (CLCA) were also identified acting on endocytosis of synaptic vesicles or receptors^{79,80} and clathrin assembly for rapid recycling of neurotransmitters.⁸¹ Beside further differentially expressed synaptic proteins, the up-regulated phosphatidylinositol transfer protein alpha isoform⁸² (PIPNA) should be mentioned because it is involved in intracellular vesicular traffic for subsequent transport processes. Proteins of the chaperone group like the mitochondrial 60 kDa heat shock protein (CH60), stress 70 protein (GRP75), T-complex protein 1 subunit beta (TCPB), Chaperonin containing Tcp1, subunit 6A (zeta 1) (CCT6A) and heat shock protein HSP 90 alpha (HS90A) are up-regulated in the lesioned striatum. The up-regulation of CH60 and GRP75 fits to the up-regulation of the mass of proteins necessary for oxidative phosphorylation in mitochondria. Moreover, TCPB up-regulation is correlated with the up-regulated actin associated proteins because it folds actin and tubulin among other cytoskeletal proteins.

Glia maturation factor beta (GMFB) is an up-regulated cell cycle protein contained in neurons and astrocytes with differentiation and regeneration functions. This up-regulation of factors converging in a proliferative pathway may suggest mitogenic or differentiative activity of a specific or different cell populations of the lesioned striatum.

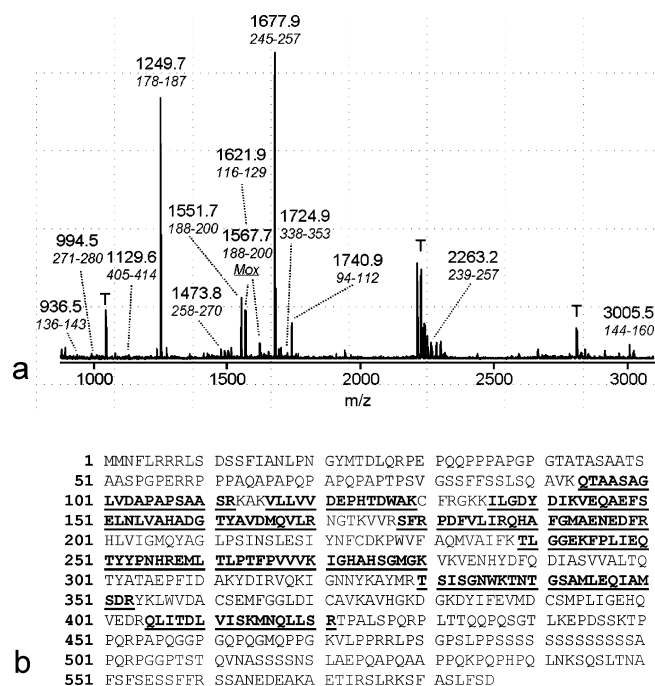


Figure 4. (a) MALDI-TOF mass spectrum from tryptic digest of synapsin-2 (SYN2). Numbers in the mass spectrum give m/z values for the detected peptide ion signals. Corresponding amino acid positions of the SYN2 amino acid sequence (Q63537) are shown in italics. Ion signals labeled with T derive from trypsin autoprolysis. (b) Amino acid sequence of SYN2_RAT. The sequence stretches that are covered by peptide ion signals (29% sequence coverage) are printed in bold letters and are underlined.

Most differentially expressed proteins of mitochondrial oxidative phosphorylation complexes (complex I–III, V) are up-regulated (Figure 6, Table 1, for specific proteins and their functions see Supporting Information) indicating an elevated requirement of energy.

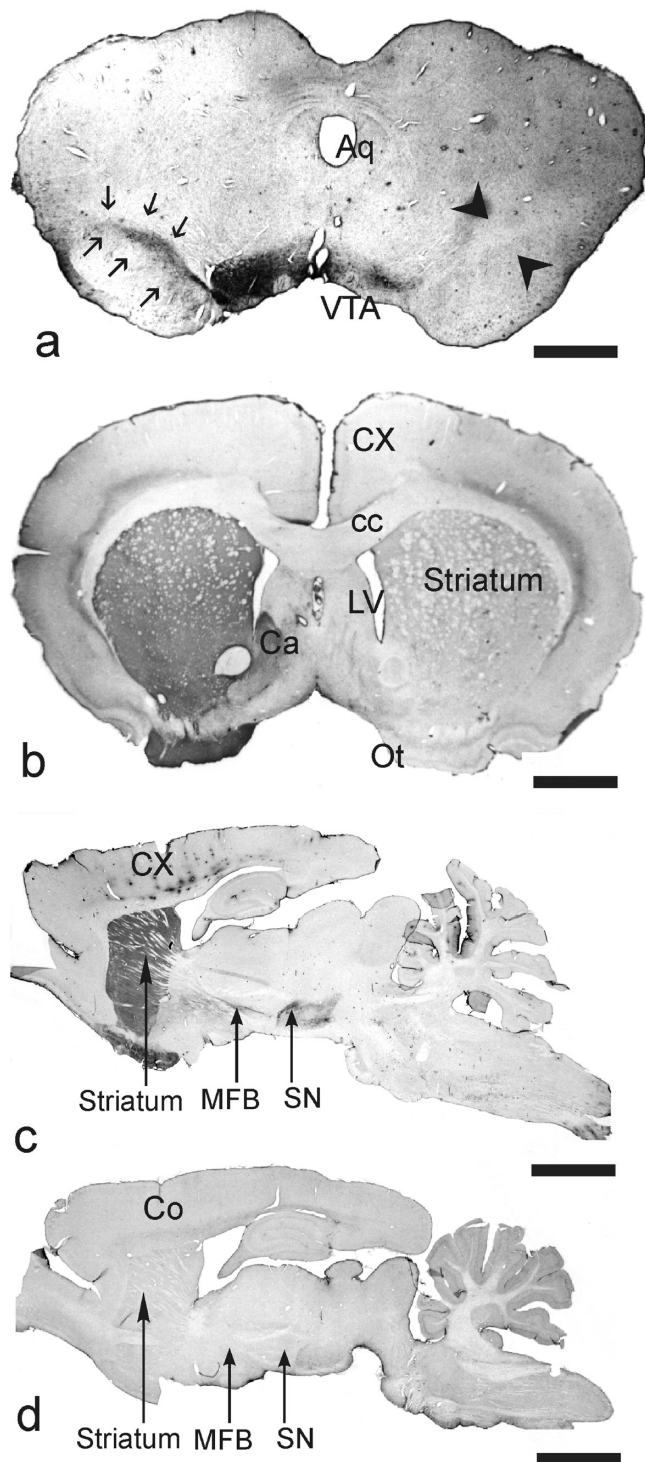


Figure 5. Immunohistochemical validation of the down-regulated TH in the striatum of 6-OHDA lesioned animals. (a) Frontal section of the mesencephalon through the SN. In the left hemisphere, TH immunoreactive neurons appear as a dark stained region (arrows). The lesioned right site do not show TH immunoreactivity. (b) Frontal section of the forebrain showing the striatum. The left control site shows strong TH immunoreactivity whereas the lesioned right site is deafferented and does not contain TH. (c) Sagittal section of a control brain showing the TH immunoreactive striatum medial forebrain bundle (MFB) and substantia nigra. (d) Sagittal section of a 6-OHDA lesioned brain without TH immunoreactive striatum and SN. Scale bars: (a): 1.0 mm, (b–d) 2.0 mm.

Proteins of the carbohydrate metabolism show elevations like the mitochondrial aconitase 2 (ACO2) and the mitochondrial isocitrate dehydrogenase (NAD) subunit beta (IDH3B) whereas the mitochondrial pyruvate dehydrogenase E1 component subunit alpha, somatic form (ODPA) and the mitochondrial malate dehydrogenase (MDHM) are down-regulated; however, the cytosolic malate dehydrogenase is not differentially expressed. Fructose-biphosphate aldolase C (ALDOC), L-lactate dehydrogenase B (LDHB) and pyruvate kinase isoenzyme M1/M2 (KPYM) are up-regulated.

The down-regulated gamma enolase (ENOG, NSE) is located in mature neurons and cells of neuronal origin. ENOG has neurotrophic and neuroprotective properties on a broad spectrum of central nervous system neurons.

Up-regulated proteins of the amino acid metabolism are aspartoacylase 2 (ACY2), cytoplasmic aspartate aminotransferase (AATC, GOT1), the mitochondrial succinatesemialdehyde dehydrogenase (SSDH), dihydrolipoyl dehydrogenase (DLDH) as part of the mitochondrial glycine cleavage system and a component of various enzyme complexes and L-glutamate dehydrogenase (DHE3) which is also a mitochondrial enzyme that has a central role in nitrogen metabolism, and catalyzes the oxidative deamination of L-glutamate to 2-oxoglutarate.⁸⁴ Glutamate is a major excitatory neurotransmitter in mammalian brains and the main substrate of DHE3. The excitatory effects of glutamate may lead to an increase of energy consumption with up-regulation of those enzymes involved in energy metabolism. Creatine kinase (KCRB), a cytoplasmic enzyme involved in energy homeostasis, is up-regulated, too. The first of three down-regulated proteins is glutamine synthetase (GLNA), a main source of energy involved in cell proliferation, inhibition of apoptosis, and cell signaling.⁸⁵ The enzyme catalyzes the synthesis of glutamine from glutamate and ammonia in astrocytes. The mitochondrial matrix Delta-1-pyrroline-5-carboxylate dehydrogenase (AL4A1) is down-regulated. AL4A1 is a NAD-dependent dehydrogenase that catalyzes the irreversible step of the proline degradation pathway, converting pyrroline-5-carboxylate to the excitatory neurotransmitter glutamate. The cytoplasmic NAD dependent deacetylase sirtuin 2 (SIRT2, sirt: (silent mating type information regulation 2, *S. cerevisiae*, homologue)) is also down-regulated.

Alterations of cofactors and proteins of vitamin metabolism have been detected. Flavin reductase or biliverdin reductase B (BLVRB) is up-regulated. It plays a possible role in protecting cells from oxidative damage or in regulating iron metabolism. The cytoplasmic pyridoxal kinase (PDXX) and pyridoxine-5'-phosphate oxidase (PNPO) are down-regulated. PNPO catalyzes the terminal, rate-limiting step in the synthesis of the biologically active form pyridoxal 5'-phosphate (P5P). P5P is a cofactor for glutamic acid decarboxylase (GAD) that decarboxylize glutamate to GABA. GABA-transaminase produces succinic semialdehyde from GABA which can be converted from SSDH (SSDH is up-regulated in the 6-OHDA lesioned striatum) to succinic acid for the TCA cycle.

An altered protein of the lipid metabolism is the up-regulated mitochondrial aldehyde dehydrogenase 2 (ALDH2). It is of particular interest because it converts aldehyde metabolites of the monoamines dopamine (DA) and serotonin (5-HT) to their acidic metabolites (3,4-dihydroxyphenylacetic acid (DOPAC), homovanillic acid (HVA), and 5-hydroxyindolacetic acid (5-HIAA)).⁸⁶ Cytosolic acyl coenzyme A thioester hydrolase or

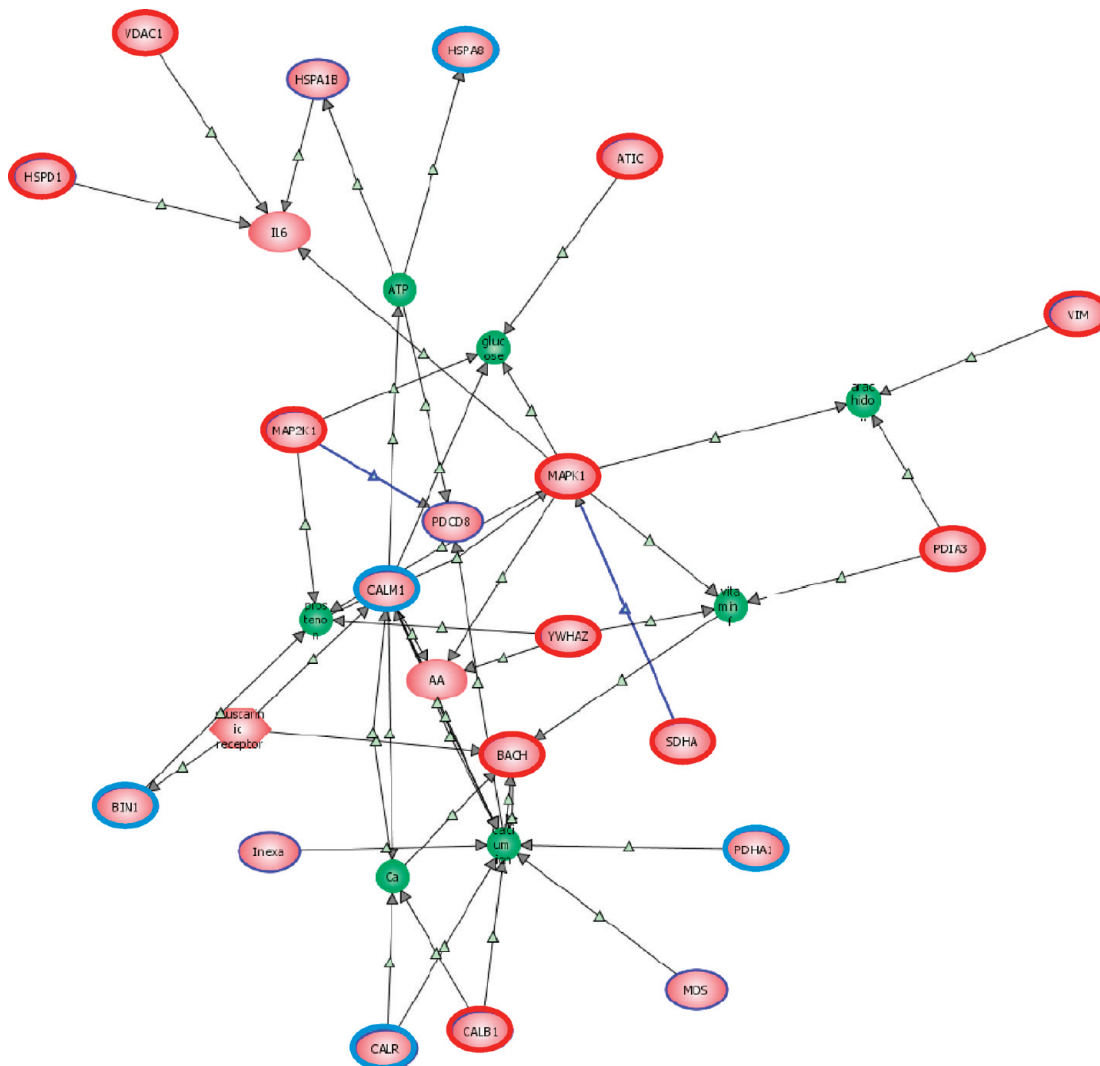


Figure 7. Proteins of calcium homeostasis CALB1, CALR, CALM1, RCN1, ANXA3, ANXA7 and their metabolic interactions are shown using Pathway Architect. The altered proteins are located in a relative small connected component of the reactome indicating close functional interactions and emphasizing their metabolic relevance in the neurotoxin altered metabolome. Blue circled, down-regulated; red circled, up-regulated.

brain acyl-CoA hydrolase (BACH) and the cytoplasmic glycerol-3-phosphate dehydrogenase 1-like protein (GPD1L) are up-regulated.

The cytosolic adenylate kinase 1 (KAD1) and biofunctional purine biosynthesis protein PURH (PUR9) were found as mixtures in spots that were up-regulated upon lesioning and play important roles in cellular energy homeostasis and nucleotide synthesis. Guanine deaminase (GUAD) is up-regulated. It is also known as a cytosolic regulator of PSD-95 postsynaptic targeting,^{88,89} matching observations of up-regulated synaptic and axonal proteins (septins, synapsin). The up-regulated inosine triphosphatase (ITPA) is located in the nuclei of neurons in the brain, prevents accumulation of inosine triphosphate and reduces the risk of incorporation of potentially mutagenic inosine nucleotides into nucleic acids.

The five proteins *N(G),N(G)*-dimethylarginin, dimethylaminotransferase 2 (DDAH2), protein disulfide isomerase (PDIA1) and protein disulfide isomerase 3 (PDIA3), mitochondrial superoxide dismutase 2 (SODM) and mitochondrial thioredoxin-dependent peroxide reductase (PRDX3) with antioxidant functions are up-regulated. The specific functions and their

relevance with regard to neurodegenerative diseases are described in the Supporting Information and partly visualized in Figure 7.

In our differential analysis the cytosolic oxygenase tyrosine hydroxylase, respectively, tyrosine-3-monooxygenase (TH) has an extremely low concentration in the lesioned striatum because the TH synthesizing neurons of the SNC have been destroyed by stereotactic 6-OHDA injection into the MFB. Hence, a down-regulation of TH in the striatal proteome matches the experiment and has been validated by immunohistochemistry (Figure 5).

Proteasomal proteins are of particular interest because their mutations lead to genetic forms of PD. Ubiquitin carboxyl terminal hydrolase L1 (UCHL1, PARK5) also known as neuron cytoplasmic protein 9.5 or PGP 9.5 is up-regulated. It is present in all neurons.⁹⁰ UCHL1 has previously been found to colocalize with parkin and α -synuclein in Lewy bodies.^{91,92} Neural F box protein 42-kDa protein (NFB42) is up-regulated, too. As a component of the SCFNFB42 E3 ubiquitin ligase it is a neuron specific protein located in all major areas of the brain.⁹³ NFB 42 contains a F box motif that couples cell cycle regulation to

the proteasome pathway.⁹⁴ The occurrence of F box in NFB42 indicates cell cycle regulation and seems to act in postmitotic neurons as a regulator for keeping them in a postmitotic state.⁹⁵

Differentially expressed proteins of signal transduction belong to the 14–3–3 protein and the guanine-nucleotide binding groups. The cytoplasmic 14-3-3 protein epsilon (1433E) and 14-3-3 protein gamma (1433G) are both down-regulated whereas 14-3-3 protein zeta (1433Z) is up-regulated. Guanine nucleotide-binding protein G(I)/G(S)/G(T) subunit beta 1 (GGB1) and guanine nucleotide-binding protein G(I)/G(S)/G(T) subunit beta 5 (GGB5) are suggested to be down-regulated, however, guanine nucleotide-binding protein G(I)/G(S)/G(T) subunit beta 2 (GGB2) is up-regulated. Guanine nucleotide-binding proteins (G proteins) are a family of proteins involved as a modulator or transducer in various transmembrane signaling systems. Some functions include activation of phospholipase A2 when bound to histamine receptors and direct opening of G-protein coupled inwardly rectifying potassium channels (GIRKs) when bound to muscarinic acetylcholine receptors. The latter function is of particular relevance for the cholinergic interneurons of the striatum. The cytoplasmic and nuclear mitogen activated protein kinase 1 (MK01) is up-regulated and occurs in degenerating neurons of PD patient brains in granules with phosphorylated extracellular signal-regulated protein kinase 1/2 (ERK1/2) localized in autophagocytosed mitochondria.⁹⁶ Dual specificity mitogen activated protein kinase kinase 1 (MP2K1) is up-regulated, too. MAP2K1 is activated when microtubule-depolymerizing agents are active (for details, see the Supporting Information).

Several proteins involved in transcription are altered. Among these, heterogeneous nuclear ribonucleoprotein A3 (ROA) and the isoform A2/B1 (ROA2) are down-regulated. HNRPs play important roles in cytoplasmic trafficking of RNA, and they are formed when nascent pre-mRNA transcripts are bound by a number of nuclear proteins forming a large multiprotein-RNA complex. Moreover, HNRPs play important roles in the splicing and transport of mRNAs and participate in early heat shock-induced splicing arrest. The down-regulation of ROA2 and ROA3 fits to the increase of DNA damage and transcription detuning due to lesioned 6-OHDA neurons and up-regulation of HNRPK indicates the involvement of striatal astrocytes through neuron-astrocyte synaptic complexes. Nucleosome assembly protein 1-like 4 (NP1L4) and RuvB-like 1 (RUVB1) are up-regulated indicating an increase of protein traffic and DNA repair processes. Importantly, transcriptional activator protein Pur-alpha (PURA) is absent in the control striatum and only expressed in the 6-OHDA lesioned striatum which is in line with the increased demand of transcription factors.

One protein with unknown or partially known function is identified. The mitochondrial precursor ES1 protein homologue (ES1) is up-regulated and contains a potential targeting sequence to mitochondria.

In conclusion, the differential analysis of control and 6-OHDA lesioned striatal proteomes points even 3 months after lesioning to massive cytoskeletal remodeling events, astrogliosis and cell proliferation with an extensive energy consumption accompanied by regulation of calcium homeostasis in parallel to protein processing by chaperones and proteasomes.

Discussion

The striatum does not consist either of a homogeneous neuron population⁹⁷ nor of a homogeneous chemoarchitecture (calbindin gradient, patch-matrix compartments)⁷¹ under spa-

tial aspects. Hence, our differential proteome investigation is a representation of overlapping spatiotemporal proteome changes. Moreover, proteins of other cell populations like neutrophils and their lactate dehydrogenase (LDH) release contain the striatal proteome. Nevertheless, proteomic approaches represent a powerful methodology to further investigate the mechanisms for understanding proteome alterations following degeneration of dopaminergic neurons and the pathophysiological events as a model for PD.⁹⁸ The separation technique used in this study allows protein separation within the range of approximately 10–100 kDa and between a pH range of 3–10. Therefore, we are able to analyze a substantial part, however, not the total proteome. It is known that a fairly large number of proteins are represented by multiple spots that may be distributed over different locations in the gel. In our studies, candidates of these distributed proteins showing a great heterogeneity belong to the families of dihydropyrimidinase related proteins, heterogeneous nuclear ribonucleoproteins, tubulin and actin.⁹⁹

Several proteins have been identified that are located in overlapping spots (Supplemental Tables 1 and 2 as well as Figure 3, Supporting Information). Hence, the results of the presented proteome analysis of the 6-OHDA lesioned striatum of the rat should be considered and interpreted as a preliminary step to elucidate the patterns of proteins differentially expressed in this neurotoxic model. To approach the analytical information that is hidden by overlapping spots several techniques for increasing protein separation at the level of 2DE,¹⁰⁰ statistical modeling of peak overlapping,¹⁰¹ more advanced identification techniques like multidimensional liquid chromatography to fractionate peptide mixtures¹⁰² need to be considered. Our differential 2D gel spot abundance analysis also does not exclude the simultaneous presence of proteins/isoforms with no detectable abundance differences but containing the same protein than that described as differential in abundance. Two up-regulated but faint spots of GRP75 (see Supplemental Table 2, Supporting Information) were found in the vicinity of an abundant nonregulated spot that represented the main component of GRP75 as was deduced from comparisons with proteome maps as well as our own unpublished results from different brain areas. These up-regulated spots apparently represented isoforms of GRP75 whose expression seems to be related to PD (see Supporting Information) while the total amount of GRP75 was rather constant. Similar results were found for alpha-internexin, 60 kDa heat shock protein, some tubulins and actin. This finding may be explained by (i) the heterogeneity of the tissue under study that contains more than one cell type, and (ii) by saturation effect of the staining procedure. Although it is often stated that multiple spots of the same protein result from different posttranslational modifications the nature of modification is seldom demonstrated. However, the present study did not characterize structural differences of the same protein in different spots. The focus of this study is layed on such protein spots that differed in abundance and give indications for cellular response to the set perturbation.

In this differential proteome study of the striatum of normal adult and 6-OHDA lesioned rats, up-regulations and down-regulations should not be related to a specific cell population (medium spiny neurons, resting or reactive astroglia, microglia endothelial cells among others) or a specific function because the dissected striata contain many cell populations and many functions at different levels of consideration. These populations

can not be differentiated after dissection within 2DE. An important aspect concerns the amount of posttranslational modifications and isoforms of differentially expressed proteins. So far, we have not investigated posttranslational modifications or specific protein groups (<10 kDa and >100 kDa (e.g., extracellular matrix proteins)). Therefore, expression levels of proteins were measured and the reasons for their changes were interpreted on a broad literature search of neurodegenerative disorders.

To reveal proteins linked to PD, gel-based approaches were used to compare the proteomic profile of human PD SN and control SN¹⁰¹. In this work, we used also protein interaction mapping of differentially expressed proteins based on the web-based interaction/pathway browsers Reactome (<http://www.reactome.org/>), ConsensusPathDB (<http://cpdb.molgen.mpg.de/>) and KEGG (<http://www.genome.jp/kegg/>).

The elevation of peroxiredoxin 2, mitochondrial complex I and III, ATP synthase,¹⁰³ and the decrease of heat shock cognate 71 kDa protein⁷² is consistent with the role of mitochondrial dysfunction and oxidative stress in PD pathogenesis. We found an up-regulation of several proteins with direct or indirect antioxidative functions (DDAH2, PDIA1, SODM, PRDX3). This can be interpreted as a protective reaction of striatal cells to oxidative stress due to microglia activation and 6-OHDA effects. Oxidation of dopamine and dopamine metabolites have also been linked to the pathology of PD.¹⁰⁴ The substantial loss of HSP7C observed in rats exposed to an oxidized product of dopamine¹⁰⁵ and the observed decrease of HSP7C in PD brains⁷² may reflect the particular susceptibility of HSP7C to dopamine oxidation. Interestingly, we measured a down-regulation of HSP7C in the 6-OHDA lesioned striatum, consistent with literature reports in rats¹⁰⁶ and mice.¹⁰⁷

A further mechanism that may affect dopaminergic neurons in PD is the rearrangement of the cytoskeleton. Proteome studies revealed that neurofilament chains are less abundant in human SN of PD patients¹⁰³ as was also found for neurofilament light polypeptide (down-regulated), and deregulation of actin cytoskeleton in a *Drosophila* PD model¹⁰⁸ and in a *C. elegans* PD model,¹⁰⁹ respectively. Our findings are in line with other models and show that several actin associated proteins have been found in the 6-OHDA lesioned striatum to be up-regulated and ACTB is down-regulated. Due to the massive dopaminergic cell death the nigrostriatal pathway must degenerate and be phagocytized by microglia. Because the striatonigral inhibitory and excitatory pathways to SN¹¹⁰ emerging from medium spiny cells do not possess DAT these axons should survive the neurotoxic trauma. However, the dopaminergic subset of targeted neurons is destroyed. It is likely that the cytoskeleton machinery is up-regulated to allow axon guidance and collateralization processes within the SN to find new postsynaptic targets. This hypothesis correlates with the up-regulation of 8 synaptic proteins necessary for synapse consolidation and synaptogenesis. Since proteins for these processes have to be synthesized in the perikaryon they are found in the striatum, a phenomenon that has been uncovered partly by our proteome study. Additional, contralateral effects could be involved as well.^{111,112} Cytoskeletal proteins of the axon and all synaptic proteins are up-regulated. The up-regulation of several proteins belonging to lipid metabolism may coincide with up-regulation of cytoskeletal proteins of axons. It is possible that these proteins are up-regulated in oligodendrocytes that synthesize myelin sheaths for the process of axon-remodeling. A further possibility is that membrane

material is synthesized in astrocytes for ensheathing processes. In contrast, the dendritic protein drebrin-like is down-regulated most probably because the presynaptic sources of the destroyed dopaminergic neurons are missing at the postsynaptic parts at the dendritic trees of medium spiny cells inducing a dendritic atrophy¹¹³ and suppression of genes encoding dendritic proteins. The impact of dendritic spines of medium spiny neurons and its prevention by L-type Ca²⁺ channel blockers after dopamine depletion in an advanced hemiparkinsonian model has been described recently.¹¹³

Both α -synuclein and parkin interact with the actin cytoskeleton^{18,114} and α -synuclein also interacts with the microtubule protein tau,¹¹⁴ reflecting their potential roles in regulating the dynamics of actin filaments and microtubules during dopaminergic degeneration.¹⁷ In a recent report of beta 3 tubulin mutations in humans the important role of TBB3/TUBB3—tubulin beta was up-regulated in our 6-OHDA lesioned striatum—with regard to axon guidance and resulting dysmorphisms of basal ganglia was emphasized.²⁰ Continued investigations to elucidate the cytoskeletal and mitochondrial changes prior to the onset of the PD may thus offer a plethora of new therapeutic strategies.

In Lewy bodies, 296 proteins were identified and as a novel component, the heat shock protein HSC70/HSP73¹¹⁵ was described. However, other heat shock proteins may be involved in dopaminergic neurons protection like the up-regulated HSP90A identified in the 6-OHDA lesioned striatum. Using a gel-based proteomic approach combined with phosphoprotein enrichment, Hong et al. found that HSP27 phosphorylation is increased in PC12 cells treated with the neurotrophic factor GDNF.¹¹⁶ Moreover, overexpression of HSP70 protects dopaminergic neurons from neurotoxicity and suppresses α -synuclein aggregation.¹¹⁷ This coincides with the up-regulated stress-induced-phosphoprotein 1 (STIP1 gene) that acts as a cochaperone reversely linking together HSP70 and HSP90.

Proteomic profiling of Parkin knockout mice, which reproduce some of the presymptomatic aspects of PD in the absence of neuronal degeneration, point to energy metabolism, stress-response chaperones and ubiquitin-proteasome pathway as possible protective mechanisms.¹¹⁸ A stress response can be presented by an up-regulation of antioxidative acting proteins like DDAH2, PDIA1, SODM and PRDX3 which were up-regulated in the 6-OHDA lesioned striatum and chaperones where STIP1, HSP90A, TCPB and CCT6A were up-regulated and HSP7C was down-regulated. The up-regulation of chaperones in the 6-OHDA lesioned striatum can be interpreted as a reaction due to a principal up-regulation of protein biosynthesis necessary for short- to long-term reorganization processes. Proteasomal proteins like stress protein 70, UCHL1 and NFB42 were up-regulated confirming observations of other reports. An important finding is the extraordinary up-regulation of mitochondrial proteins directly or indirectly involved in energy metabolism correlating with earlier findings measuring the glucose utilization in the striatum of 6-OHDA lesioned rats.¹¹⁹ In our model, this can be explained by a general larger requirement for ATP because many new structural proteins are synthesized and therefore pointing to a metabolic pattern with up-regulation of nucleic acid metabolism, transcriptional factors, chaperones to control the structure of these new proteins (axonal cytoskeleton proteins, actin associated proteins, synaptic proteins) and proteasomal proteins. Microglial activation following the initial neurodegeneration may subsequently enhance the degenerative process. Bioactive substances re-

leased by degenerating dopaminergic neurons,¹¹⁷ including aggregated α -synuclein¹²⁰ are known to activate microglia.¹¹⁷ Proteomic profiling of microglia exposed to nitrated and aggregated α -synuclein identified inflammatory proteins, indicating the important role of secondary neuroinflammation in the progression of nigral degeneration and PD.¹²¹ However, up-regulation of inflammation-related proteins in proteome analyses have been shown to occur in many studies independent of the model system.^{122–125} In our study, we have not found direct hints pointing to inflammatory processes. However, this can be due to the time point of 3 months after the 6-OHDA lesion had been performed, and, perhaps even more likely, to the long spatial distance between the perturbed brain region (substantia nigra) and the analyzed brain region (striatum).

Many differentially expressed proteins are localized in the mitochondrial compartment and most of them are necessary for energy metabolism in the TCA cycle and oxidative phosphorylation (Figure 6). Along with molecules of ATP synthesis, mitochondrial VDAC1 and CH60 are also up-regulated (Figure 6). These findings indicate a strong requirement of energy, respectively, ATP. Mitochondria are involved in excitotoxic damage of nerve cells. Following the breakdown of the calcium-buffering ability of mitochondria, mitochondrial calcium overload induces reactive oxygen species (ROS) bursts that produce free radicals and open permeability transition pores, ultimately leading to neuronal cell death. We found an up-regulation of several proteins assuring calcium homeostasis whereas calmodulin, calreticulin and reticulocalbin 1 are down-regulated (Figure 7). The main calcium storage of neurons is the ER, however, high calcium concentrations in mitochondria are necessary for Ca^{2+} dependent enzymes, for example, glycogen phosphorylase. An up-regulation of proteins of energy metabolism coincides with the measured up-regulation of proteins involved in calcium homeostasis. Moreover, all identified proteins with antioxidative functions are up-regulated. They are involved in counteracting ROS neutralization whereas the increase of ROS generation may originate from the higher energy demand for the observed cytoskeletal remodeling. Subsequently proteins involved in antioxidation can be up-regulated as found here. Our data support an upstream role for mitochondrial dysfunction of the 6-OHDA lesion of the striatum similar to PD.

Alterations of protein expressions referring to organizing calcium homeostasis were found pointing to regulatory needs of cytoplasmic and mitochondrial Ca^{2+} concentrations and ER Ca^{2+} storage in environment of strong cytoplasmic-extracellular- Ca^{2+} -gradients.

The overall up-regulation of proteins should lead to an up-regulation of transcriptional proteins. Indeed we observed an up-regulation of nucleosome assembly proteins 1-like 4 and RuvB like 1. However, the transcriptional activator protein Pur-alpha was absent in the control striatum that could be explained by reducing astrogliosis and/or microglia activity. We suggest that the up-regulation of nucleic acid metabolism is pointing to cell cycle events like DNA reduplication and mitosis of astrocytes and microglia to support astrogliosis induced by nigrostriatal deafferentiation.

An indirect indication of astrogliosis is the up-regulation of the astrocytic cytoskeletal protein vimentin correlating with other studies.^{126,127} In line with up-regulation of transcriptional, astrocyte cytoskeletal proteins and nucleic acid metabolism is the observation that proteins of cell differentiation and pro-

liferation like glial maturation factor beta and *N*-acetylneuraminic acid synthase are also up-regulated. Some of the 14-3-3 signal transduction proteins for cell division, differentiation, apoptosis and neurotransmission (TH activation) are up- and down-regulated. The up-regulation of 14-3-3Z coincides with the up-regulation of the mitochondrial CH60 chaperone. In the 6-OHDA lesioned striatum MAP kinases 1 and/or 2 are up-regulated and are also involved in proliferation and differentiation processes. The GTPases GBB1 and 5 are involved in second messenger signal transmission and are down-regulated. Because the nigrostriatal inputs to medium spiny neurons are destroyed these neurons receive no or less dopaminergic induced postsynaptic activation and may down-regulate their GTPase activity.

In conclusion, the neurotoxin induced proteome alterations that were studied here indicate vivid long-distance remodeling processes of dendrites, axons and synapses that are still ongoing in the striatum even three months after lesioning of neurons from the substantia nigra. The heavy metabolic activities are indicating a high plasticity and regeneration potential in the adult rat brain.

Abbreviations (for abbreviations of further proteins see Table 1): 2DE, 2-dimensional polyacrylamide gel electrophoresis; 6-OHDA, 6-hydroxydopamine; 6-OHDOPA, 6-hydroxydopa; BW, body weight; cc, Corpus callosum; CHAPS, 3-[(3-cholamidopropyl)dimethylammonio]-1-propanesulfonate; CHCA, α -cyano-4-hydroxycinnamic acid; CNS, central nervous system; CX, Cortex cerebri; D1, dopamine 1 receptor; D2, dopamine 2 receptor; DA, dopamine; DAT, dopamine transporter; 2DE, two-dimensional electrophoresis; DTT, dithiothreitol; GDNF, glial cell line-derived neurotrophic factor; GSH, glutathione; IEF, isoelectric focusing; IL-1beta, interleukin 1 beta; i.p., intraperitoneal; IPG, immobilized pH gradient; MALDI-TOF, matrix assisted laser desorption/ionization time-of-flight; MFB, medial forebrain bundle; MPTP, 1-methyl-4-phenyl-1,2,3,6-tetrahydropyridine; MS, mass spectrometry; NF, neurofilament; PBS, phosphate buffered saline; PD, Parkinson's disease; PMF, peptide mass fingerprint; PMSF, phenylmethylsulfonyl-fluoride; PSD-95, postsynaptic density protein 95; ROS, reactive oxygen species; s.c., subcutan; SEM, standard error of mean; SN, substantia nigra; SNC, substantia nigra pars compacta; TCA, Tricarboxylic acid cycle; TH, tyrosine hydroxylase = tyrosine-3-monooxygenase; TNFalpha, tumor necrosis factor alpha.

Acknowledgment. We thank Antje Schumann for substantial laboratory work, Manuela Sieb for technical hints and Dr. Dirk Koczan for giving advices for pathway analysis.

Supporting Information Available: Appendix and Supplemental tables and figures. This material is available free of charge via the Internet at <http://pubs.acs.org>.

References

- (1) Forno, L. S. Neuropathology of Parkinson's disease. *J. Neuro-pathol. Exp. Neurol.* **1996**, *55* (3), 259–72.
- (2) Lang, A. E.; Lozano, A. M. Parkinson's disease. Second of two parts. *N. Engl. J. Med.* **1998**, *339* (16), 1130–43.
- (3) Lang, A. E.; Lozano, A. M. Parkinson's disease. First of two parts. *N. Engl. J. Med.* **1998**, *339* (15), 1044–53.
- (4) Blandini, F.; Nappi, G.; Tassorelli, C.; Martignoni, E. Functional changes of the basal ganglia circuitry in Parkinson's disease. *Prog. Neurobiol.* **2000**, *62* (1), 63–88.
- (5) Nakano, I.; Fujimoto, K. [Rating scale and functional prognosis of Parkinson's disease]. *Nippon Rinsho.* **2000**, *58* (10), 2132–8.

- (6) Cookson, M. R. Parkin's substrates and the pathways leading to neuronal damage. *Neuromol. Med.* **2003**, 3 (1), 1–13.
- (7) Eriksen, J. L.; Wszolek, Z.; Petrucelli, L. Molecular pathogenesis of Parkinson disease. *Arch. Neurol.* **2005**, 62 (3), 353–7.
- (8) Jeon, B. S.; Jackson-Lewis, V.; Burke, R. E. 6-Hydroxydopamine lesion of the rat substantia nigra: time course and morphology of cell death. *Neurodegeneration* **1995**, 4 (2), 131–7.
- (9) Graeber, M. B.; Grashon-Frodl, E.; Abell-Aleff, P.; Kosel, S. Nigral neurons are likely to die of a mechanism other than classical apoptosis in Parkinson's disease. *Parkinsonism Relat. Disord.* **1999**, 5 (4), 187–92.
- (10) Bove, J.; Prou, D.; Perier, C.; Przedborski, S. Toxin-induced models of Parkinson's disease. *NeuroRx* **2005**, 2 (3), 484–94.
- (11) Miller, R. L.; James-Kravage, M.; Sun, G. Y.; Sun, A. Y. Oxidative and inflammatory pathways in Parkinson's disease. *Neurochem. Res.* **2009**, 34 (1), 55–65.
- (12) Faull, R. L.; Laverty, R. Changes in dopamine levels in the corpus striatum following lesions in the substantia nigra. *Exp. Neurol.* **1969**, 23 (3), 332–40.
- (13) Deumens, R.; Blokland, A.; Prickaerts, J. Modeling Parkinson's disease in rats: an evaluation of 6-OHDA lesions of the nigrostriatal pathway. *Exp. Neurol.* **2002**, 175 (2), 303–17.
- (14) Sauer, H.; Oertel, W. H. Progressive degeneration of nigrostriatal dopamine neurons following intrastriatal terminal lesions with 6-hydroxydopamine: a combined retrograde tracing and immunocytochemical study in the rat. *Neuroscience* **1994**, 59 (2), 401–15.
- (15) Chin, M. H.; Qian, W. J.; Wang, H.; Petyuk, V. A.; Bloom, J. S.; Sforza, D. M.; Lacan, G.; Liu, D.; Khan, A. H.; Cantor, R. M.; Bigelow, D. J.; Melega, W. P.; Camp, D. G., 2nd; Smith, R. D.; Smith, D. J. Mitochondrial dysfunction, oxidative stress, and apoptosis revealed by proteomic and transcriptomic analyses of the striata in two mouse models of Parkinson's disease. *J. Proteome Res.* **2008**, 7 (2), 666–77.
- (16) Zhang, X.; Zhou, J. Y.; Chin, M. H.; Schepmoes, A. A.; Petyuk, V. A.; Weitz, K. K.; Petritis, B. O.; Monroe, M. E.; Camp, D. G.; Wood, S. A.; Melega, W. P.; Bigelow, D. J.; Smith, D. J.; Qian, W. J.; Smith, R. D. Region-specific protein abundance changes in the brain of MPTP-induced Parkinson's disease mouse model. *J. Proteome Res.* **2010**, 9 (3), 1496–509.
- (17) Sousa, V. L.; Bellani, S.; Giannandrea, M.; Yousuf, M.; Valtorta, F.; Meldolesi, J.; Chieregatti, E. α -synuclein and its A30P mutant affect actin cytoskeletal structure and dynamics. *Mol. Biol. Cell* **2009**, 20 (16), 3725–39.
- (18) Huynh, D. P.; Scoles, D. R.; Ho, T. H.; Del Bigio, M. R.; Pulst, S. M. Parkin is associated with actin filaments in neuronal and nonneuronal cells. *Ann. Neurol.* **2000**, 48 (5), 737–44.
- (19) McFarland, M. A.; Ellis, C. E.; Markey, S. P.; Nussbaum, R. L. Proteomics analysis identifies phosphorylation-dependent α -synuclein protein interactions. *Mol. Cell. Proteomics* **2008**, 7 (11), 2123–37.
- (20) Tischfield, M. A.; Baris, H. N.; Wu, C.; Rudolph, G.; Van Maldergem, L.; He, W.; Chan, W.-M.; Andrews, C.; Demer, J. L.; Robertson, R. L.; Mackey, D. A.; Ruddle, J. B.; Bird, T. D.; Gottlob, I.; Pieh, C.; Traboulsi, E. I.; Pomeroy, S. L.; Hunter, D. G.; Soul, J. S.; Newlin, A.; Sabol, L. J.; Doherty, E. J.; de Uzcátegui, C. E.; de Uzcátegui, N.; Collins, M. L. Z.; Sener, E. C.; Wabbels, B.; Hellebrand, H.; Meitinger, T.; de Berardinis, T.; Magli, A.; Schiavi, C.; Pastore-Trossello, M.; Koc, F.; Wong, A. M.; Levin, A. V.; Geraghty, M. T.; Descartes, M.; Flaherty, M.; Jamieson, R. V.; Möller, H. U.; Meuthen, I.; Callen, D. F.; Kerwin, J.; Lindsay, S.; Meindl, A.; Guptasand, M. L.; Pellman, D.; Engle, E. C. Human TUBB3 mutations perturb microtubule dynamics, kinesin interactions, and axon guidance. *Cell* **2010**, 140 (1), 74–87.
- (21) Yates, D. M.; Manser, C.; De Vos, K. J.; Shaw, C. E.; McLoughlin, D. M.; Miller, C. C. Neurofilament subunit (NFL) head domain phosphorylation regulates axonal transport of neurofilaments. *Eur. J. Cell Biol.* **2009**, 88 (4), 193–202.
- (22) Petzold, A.; Altintas, A.; Andreoni, L.; Bartos, A.; Berthele, A.; Blankenstein, M. A.; Buee, L.; Castellazzi, M.; Cepok, S.; Comabella, M.; Constantinescu, C. S.; Deisenhammer, F.; Deniz, G.; Erten, G.; Espino, M.; Fainardi, E.; Franciotta, D.; Freedman, M. S.; Giedraitis, V.; Gilhus, N. E.; Giovannoni, G.; Glabinski, A.; Grieb, P.; Hartung, H. P.; Hemmer, B.; Herukka, S. K.; Hintzen, R.; Ingelsson, M.; Jackson, S.; Jacobsen, S.; Jafari, N.; Jalosinski, M.; Jarius, S.; Kapaki, E.; Kieseier, B. C.; Koel-Simmelink, M. J.; Kornhuber, J.; Kuhle, J.; Kurzepa, J.; Lalive, P. H.; Lannfelt, L.; Lehmsiek, V.; Lewczuk, P.; Livrea, P.; Marnetto, F.; Martino, D.; Menge, T.; Norgren, N.; Papuc, E.; Paraskevas, G. P.; Pirttila, T.; Rajda, C.; Rejdak, K.; Ricny, J.; Ripova, D.; Rosengren, L.; Ruggieri, M.; Schraen, S.; Shaw, G.; Sindic, C.; Siva, A.; Stigbrand, T.; Stonebridge, I.; Topcular, B.; Trojano, M.; Tumani, H.; Twaalfhoven, H. A.; Vecsei, L.; Van Pesch, V.; Vanderstichele, H.; Vedeler, C.; Verbeek, M. M.; Villar, L. M.; Weissert, R.; Wildemann, B.; Yang, C.; Yao, K.; Teunissen, C. E. Neurofilament ELISA validation. *J. Immunol. Methods* **2009**.
- (23) Butkevich, E.; Hulsmann, S.; Wenzel, D.; Shirao, T.; Duden, R.; Majoul, I. Drebrin is a novel connexin-43 binding partner that links gap junctions to the submembrane cytoskeleton. *Curr. Biol.* **2004**, 14 (8), 650–8.
- (24) Betarbet, R.; Sherer, T. B.; Greenamyre, J. T. Animal models of Parkinson's disease. *Bioessays* **2002**, 24 (4), 308–18.
- (25) Schober, A. Classic toxin-induced animal models of Parkinson's disease: 6-OHDA and MPTP. *Cell Tissue Res.* **2004**, 318 (1), 215–24.
- (26) Somayajulu-Nitu, M.; Sandhu, J. K.; Cohen, J.; Sikorska, M.; Sridhar, T. S.; Matei, A.; Borowy-Borowski, H.; Pandey, S. Paraquat induces oxidative stress, neuronal loss in substantia nigra region and parkinsonism in adult rats: neuroprotection and amelioration of symptoms by water-soluble formulation of coenzyme Q10. *BMC Neurosci.* **2009**, 10, 88.
- (27) Xiong, N.; Huang, J.; Zhang, Z.; Zhang, Z.; Xiong, J.; Liu, X.; Jia, M.; Wang, F.; Chen, C.; Cao, X.; Liang, Z.; Sun, S.; Lin, Z.; Wang, T. Stereotaxical infusion of rotenone: a reliable rodent model for Parkinson's disease. *PLoS One* **2009**, 4 (11), e7878.
- (28) Schmidt, W. J.; Alam, M. Controversies on new animal models of Parkinson's disease pro and con: the rotenone model of Parkinson's disease (PD). *J. Neural Transm. Suppl.* **2006**, (70), 273–6.
- (29) Hawlitschka, A.; Haas, S. J.; Schmitt, O.; Weiss, D. G.; Wree, A. Effects of systemic PSI administration on catecholaminergic cells in the brain, adrenal medulla and carotid body in Wistar rats. *Brain Res.* **2007**, 1173, 137–44.
- (30) Isacson, O.; Kordower, J. H. Future of cell and gene therapies for Parkinson's disease. *Ann. Neurol.* **2008**, 64 (2), S122–38.
- (31) Cai, J.; Donaldson, A.; Yang, M.; German, M. S.; Enkolopov, G.; Iacovitti, L. The role of Lmx1a in the differentiation of human embryonic stem cells into midbrain dopamine neurons in culture and after transplantation into a Parkinson's disease model. *Stem Cells* **2009**, 27 (1), 220–9.
- (32) Hess, D. C.; Borlongan, C. V. Stem cells and neurological diseases. *Cell Prolif.* **2008**, 41, 94–114.
- (33) Ebert, A. D.; Beres, A. J.; Barber, A. E.; Svendsen, C. N. Human neural progenitor cells over-expressing IGF-1 protect dopamine neurons and restore function in a rat model of Parkinson's disease. *Exp. Neurol.* **2008**, 209 (1), 213–23.
- (34) Redmond, D. E., Jr.; Bjugstad, K. B.; Teng, Y. D.; Ourednik, V.; Ourednik, J.; Wakeman, D. R.; Parsons, X. H.; Gonzalez, R.; Blanchard, B. C.; Kim, S. U.; Gu, Z.; Lipton, S. A.; Markakis, E. A.; Roth, R. H.; Elsworth, J. D.; Sladek, J. R., Jr.; Sidman, R. L.; Snyder, E. Y. Behavioral improvement in a primate Parkinson's model is associated with multiple homeostatic effects of human neural stem cells. *Proc. Natl. Acad. Sci. U.S.A.* **2007**, 104 (29), 12175–80.
- (35) Hovakimyan, M.; Haas, S. J.; Schmitt, O.; Gerber, B.; Wree, A.; Andressen, C. Mesencephalic human neural progenitor cells transplanted into the neonatal hemiparkinsonian rat striatum differentiate into neurons and improve motor behaviour. *J. Anat.* **2006**, 209 (6), 721–32.
- (36) Fillmore, H. L.; Holloway, K. L.; Gillies, G. T. Cell replacement efforts to repair neuronal injury: a potential paradigm for the treatment of Parkinson's disease. *NeuroRehabilitation* **2005**, 20 (3), 233–42.
- (37) Goldman, S. Stem and progenitor cell-based therapy of the human central nervous system. *Nat. Biotechnol.* **2005**, 23 (7), 862–71.
- (38) Sun, F.; Cavalli, V. Neuroproteomics: towards understanding neuronal regeneration and degeneration. *Mol. Cell. Proteomics* **2009**.
- (39) Fountoulakis, M.; Tsangaris, G. T.; Maris, A.; Lubec, G. The rat brain hippocampus proteome. *J. Chromatogr., B: Analyt. Technol. Biomed. Life Sci.* **2005**, 819 (1), 115–29.
- (40) Kanehisa, M.; Goto, S. KEGG: Kyoto encyclopedia of genes and genomes. *Nucleic Acids Res.* **2000**, 28 (1), 27–30.
- (41) Kanehisa, M.; Goto, S.; Furumichi, M.; Tanabe, M.; Hirakawa, M. KEGG for representation and analysis of molecular networks involving diseases and drugs. *Nucleic Acids Res.* (n/a), 38 (Database issue), D355–60.
- (42) Kanehisa, M.; Goto, S.; Hattori, M.; Aoki-Kinoshita, K. F.; Itoh, M.; Kawashima, S.; Katayama, T.; Araki, M.; Hirakawa, M. From genomics to chemical genomics: new developments in KEGG. *Nucleic Acids Res.* **2006**, 34 (Database issue), D354–7.

- (43) Paxinos, G.; Watson, C. *The rat brain in stereotaxic coordinates*, 6th ed.; Elsevier: Amsterdam, 2007.
- (44) Hefti, F.; Melamed, E.; Sahakian, B. J.; Wurtman, R. J. Circling behavior in rats with partial, unilateral nigro-striatal lesions: effect of amphetamine, apomorphine, and DOPA. *Pharmacol., Biochem. Behav.* **1980**, *12* (2), 185–8.
- (45) Hefti, F.; Melamed, E.; Wurtman, R. J. Partial lesions of the dopaminergic nigrostriatal system in rat brain: biochemical characterization. *Brain Res.* **1980**, *195* (1), 123–37.
- (46) Heikkila, R. E.; Shapiro, B. S.; Duvoisin, R. C. The relationship between loss of dopamine nerve terminals, striatal [3H]spiroperidol binding and rotational behavior in unilaterally 6-hydroxydopamine-lesioned rats. *Brain Res.* **1981**, *211* (2), 285–92.
- (47) Casas, M.; Guix, T.; Prat, G.; Ferre, S.; Cadafalch, J.; Jane, F. Conditioning of rotational behavior after the administration of a single dose of apomorphine in rats with unilateral denervation of the dopaminergic nigrostriatal pathway: relevance to drug addiction. *Pharmacol., Biochem. Behav.* **1988**, *31* (3), 605–9.
- (48) Carman, L. S.; Gage, F. H.; Shults, C. W. Partial lesion of the substantia nigra: relation between extent of lesion and rotational behavior. *Brain Res.* **1991**, *553* (2), 275–83.
- (49) Hudson, J. L.; van Horne, C. G.; Stromberg, I.; Brock, S.; Clayton, J.; Masserano, J.; Hoffer, B. J.; Gerhardt, G. A. Correlation of apomorphine- and amphetamine-induced turning with nigrostriatal dopamine content in unilaterally 6-hydroxydopamine lesioned rats. *Brain Res.* **1993**, *626* (1–2), 167–74.
- (50) Moore, A. E.; Cicchetti, F.; Hennen, J.; Isacson, O. Parkinsonian motor deficits are reflected by proportional A9/A10 dopamine neuron degeneration in the rat. *Exp. Neurol.* **2001**, *172* (2), 363–76.
- (51) Ungerstedt, U.; Arbuthnott, G. W. Quantitative recording of rotational behavior in rats after 6-hydroxy-dopamine lesions of the nigrostriatal dopamine system. *Brain Res.* **1970**, *24* (3), 485–93.
- (52) Zetterstrom, T.; Herrera-Marschitz, M.; Ungerstedt, U. Simultaneous measurement of dopamine release and rotational behaviour in 6-hydroxydopamine denervated rats using intracerebral dialysis. *Brain Res.* **1986**, *376* (1), 1–7.
- (53) Schmidt, R. H.; Ingvar, M.; Lindvall, O.; Stenevi, U.; Bjorklund, A. Functional activity of substantia nigra grafts reinnervating the striatum: neurotransmitter metabolism and [14C]2-deoxy-D-glucose autoradiography. *J. Neurochem.* **1982**, *38* (3), 737–48.
- (54) Carta, M.; Lindgren, H. S.; Lundblad, M.; Stancampiano, R.; Fadda, F.; Cenci, M. A. Role of striatal L-DOPA in the production of dyskinesia in 6-hydroxydopamine lesioned rats. *J. Neurochem.* **2006**, *96* (6), 1718–27.
- (55) Lorenz, P.; Bantscheff, M.; Ibrahim, S. M.; Thiesen, H. J.; Glocker, M. O. Proteome analysis of diseased joints from mice suffering from collagen-induced arthritis. *Clin. Chem. Lab. Med.* **2003**, *41* (12), 1622–32.
- (56) Just, T.; Gafumbegete, E.; Gramberg, J.; Pruffer, I.; Mikkat, S.; Ringel, B.; Pau, H. W.; Glocker, M. O. Differential proteome analysis of tonsils from children with chronic tonsillitis or with hyperplasia reveals disease-associated protein expression differences. *Anal. Bioanal. Chem.* **2006**, *384* (5), 1134–44.
- (57) Rower, C.; Vissers, J. P.; Koy, C.; Kipping, M.; Hecker, M.; Reimer, T.; Gerber, B.; Thiesen, H. J.; Glocker, M. O. Towards a proteome signature for invasive ductal breast carcinoma derived from label-free nanoscale LC-MS protein expression profiling of tumorous and glandular tissue. *Anal. Bioanal. Chem.* **2009**, *395* (8), 2443–56.
- (58) Bradford, M. M. A rapid and sensitive method for the quantitation of microgram quantities of protein utilizing the principle of protein-dye binding. *Anal. Biochem.* **1976**, *72*, 248–54.
- (59) Görg, A. P.; W; Friedrich, C.; Kuick, R.; Strahler, J. R.; Hanash, S. M. Temperature-dependent spot positional variability in two-dimensional polypeptide patterns. *Electrophoresis* **1991**, *12*, 653–658.
- (60) Görg, A. W. W.; Dunn, M. J. Current two-dimensional electrophoresis technology for proteomics. *Proteomics* **2004**, *4*, 3665–3685.
- (61) Westermeier, R. Sensitive, quantitative, and fast modifications for Coomassie Blue staining of polyacrylamide gels. *Proteomics* **2006**, *6* (2), 61–4.
- (62) Bantscheff, M.; Ringel, B.; Madi, A.; Schnabel, R.; Glocker, M. O.; Thiesen, H. J. Differential proteome analysis and mass spectrometric characterization of germ line development-related proteins of *Caenorhabditis elegans*. *Proteomics* **2004**, *4* (8), 2283–95.
- (63) Li, Z.; Kreutzer, M.; Mikkat, S.; Mise, N.; Glocker, M. O.; Putzer, B. M. Proteomic analysis of the E2F1 response in p53-negative cancer cells: new aspects in the regulation of cell survival and death. *Proteomics* **2006**, *6* (21), 5735–45.
- (64) Fulda, S.; Mikkat, S.; Huang, F.; Huckauf, J.; Marin, K.; Norling, B.; Hagemann, M. Proteomic analysis of salt stress response in the cyanobacterium *Synechocystis* sp. strain PCC 6803. *Proteomics* **2006**, *6* (9), 2733–45.
- (65) Nordhoff, E.; Schürenberg, M.; Thiele, G.; Lübbert, C.; Kloeppel, I. K.-D.; Theiss, D.; Lehrach, H.; Gobom, J. Sample preparation protocols for MALDI-MS of peptides and oligonucleotides using prestructured sample supports. *Int. J. Mass Spectrom.* **2003**, *226*, 163–180.
- (66) Mikkat, S.; Koy, C.; Ulbrich, M.; Ringel, B.; Glocker, M. O. Mass spectrometric protein structure characterization reveals cause of migration differences of haptoglobin alpha chains in two-dimensional gel electrophoresis. *Proteomics* **2004**, *4* (12), 3921–32.
- (67) Heitner, J. C.; Koy, C.; Kreutzer, M.; Gerber, B.; Reimer, T.; Glocker, M. O. Differentiation of HELLP patients from healthy pregnant women by proteome analysis--on the way towards a clinical marker set. *J. Chromatogr., B: Analyt. Technol. Biomed. Life Sci.* **2006**, *840* (1), 10–9.
- (68) Aminin, D. L.; Koy, C.; Dmitrenok, P. S.; Muller-Hilke, B.; Koczan, D.; Arbogast, B.; Silchenko, A. A.; Kalinin, V. I.; Avilov, S. A.; Stonik, V. A.; Collin, P. D.; Thiesen, H. J.; Deinzer, M. L.; Glocker, M. O. Immunomodulatory effects of holothurian triterpene glycosides on mammalian splenocytes determined by mass spectrometric proteome analysis. *J. Proteomics* **2009**, *72* (5), 886–906.
- (69) Petrak, J.; Ivanek, R.; Toman, O.; Cmejla, R.; Cmejlova, J.; Vyoral, D.; Zivny, J.; Vulpe, C. D. Deja vu in proteomics. A hit parade of repeatedly identified differentially expressed proteins. *Proteomics* **2008**, *8* (9), 1744–9.
- (70) Wang, P.; Bouwman, F. G.; Mariman, E. C. Generally detected proteins in comparative proteomics--a matter of cellular stress response. *Proteomics* **2009**, *9* (11), 2955–66.
- (71) Gerfen, C. R. Basal ganglia. In *The Rat Nervous System*, 3rd ed.; Paxinos, G., Ed.; Elsevier Academic Press: Amsterdam, 2004; pp 455–508.
- (72) Jin, J.; Hulette, C.; Wang, Y.; Zhang, T.; Pan, C.; Wadhwa, R.; Zhang, J. Proteomic identification of a stress protein, mortalin/mthsp70/GRP75: relevance to Parkinson disease. *Mol. Cell. Proteomics* **2006**, *5* (7), 1193–204.
- (73) Jimenez, C. R.; Stam, F. J.; Li, K. W.; Gouwenberg, Y.; Hornshaw, M. P.; De Winter, F.; Verhaagen, J.; Smit, A. B. Proteomics of the injured rat sciatic nerve reveals protein expression dynamics during regeneration. *Mol. Cell. Proteomics* **2005**, *4* (2), 120–32.
- (74) Fukuda, T.; Oyamada, H.; Isshiki, T.; Maeda, M.; Kusakabe, T.; Hozumi, A.; Yamaguchi, T.; Igarashi, T.; Hasegawa, H.; Seidoh, T.; Suzuki, T. Distribution and variable expression of secretory pathway protein reticulocalbin in normal human organs and non-neoplastic pathological conditions. *J. Histochem. Cytochem.* **2007**, *55* (4), 335–45.
- (75) Mizrak, S. C.; Bogerd, J.; Lopez-Casas, P. P.; Parraga, M.; Del Mazo, J.; de Rooij, D. G. Expression of stress inducible protein 1 (Stip1) in the mouse testis. *Mol. Reprod. Dev.* **2006**, *73* (11), 1361–6.
- (76) Li, K. W.; Hornshaw, M. P.; Van Der Schors, R. C.; Watson, R.; Tate, S.; Casetta, B.; Jimenez, C. R.; Gouwenberg, Y.; Gundelfinger, E. D.; Smalla, K. H.; Smit, A. B. Proteomics analysis of rat brain postsynaptic density. Implications of the diverse protein functional groups for the integration of synaptic physiology. *J. Biol. Chem.* **2004**, *279* (2), 987–1002.
- (77) Ding, Q.; Vaynman, S.; Souda, P.; Whitelegge, J. P.; Gomez-Pinilla, F. Exercise affects energy metabolism and neural plasticity-related proteins in the hippocampus as revealed by proteomic analysis. *Eur. J. Neurosci.* **2006**, *24* (5), 1265–76.
- (78) Shi, M.; Bradner, J.; Bammler, T. K.; Eaton, D. L.; Zhang, J.; Ye, Z.; Wilson, A. M.; Montine, T. J.; Pan, C.; Zhang, J. Identification of glutathione S-transferase pi as a protein involved in Parkinson disease progression. *Am. J. Pathol.* **2009**, *175* (1), 54–65.
- (79) Ritter, B.; Blondeau, F.; Denisov, A. Y.; Gehring, K.; McPherson, P. S. Molecular mechanisms in clathrin-mediated membrane budding revealed through subcellular proteomics. *Biochem. Soc. Trans.* **2004**, *32* (Pt 5), 769–73.
- (80) Murshid, A.; Srivastava, A.; Kumar, R.; Presley, J. F. Characterization of the localization and function of NECAP 1 in neurons. *J. Neurochem.* **2006**, *98* (6), 1746–62.
- (81) Conner, S. D.; Schmid, S. L. Regulated portals of entry into the cell. *Nature* **2003**, *422* (6927), 37–44.
- (82) Hay, J. C.; Martin, T. F. Phosphatidylinositol transfer protein required for ATP-dependent priming of Ca(2+)-activated secretion. *Nature* **1993**, *366* (6455), 572–5.

- (83) Liscovitch, M.; Cantley, L. C. Signal transduction and membrane traffic: the P13K/phosphoinositide connection. *Cell* **1995**, *81* (5), 659–62.
- (84) Smith, T. J.; Peterson, P. E.; Schmidt, T.; Fang, J.; Stanley, C. A. Structures of bovine glutamate dehydrogenase complexes elucidate the mechanism of purine regulation. *J. Mol. Biol.* **2001**, *307* (2), 707–20.
- (85) Haberle, J.; Gorg, B.; Rutsch, F.; Schmidt, E.; Toutain, A.; Benoist, J. F.; Gelot, A.; Suc, A. L.; Hohne, W.; Schliess, F.; Haussinger, D.; Koch, H. G. Congenital glutamine deficiency with glutamine synthetase mutations. *N. Engl. J. Med.* **2005**, *353* (18), 1926–33.
- (86) Fernandez, E.; Koek, W.; Ran, Q.; Gerhardt, G. A.; France, C. P.; Strong, R. Monoamine metabolism and behavioral responses to ethanol in mitochondrial aldehyde dehydrogenase knockout mice. *Alcohol.: Clin. Exp. Res.* **2006**, *30* (10), 1650–8.
- (87) Gravel, M.; Peterson, J.; Yong, V. W.; Kottis, V.; Trapp, B.; Braun, P. E. Overexpression of 2',3'-cyclic nucleotide 3'-phosphodiesterase in transgenic mice alters oligodendrocyte development and produces aberrant myelination. *Mol. Cell. Neurosci.* **1996**, *7* (6), 453–66.
- (88) Riefler, G. M.; Balasingam, G.; Lucas, K. G.; Wang, S.; Hsu, S. C.; Firestein, B. L. Exocyst complex subunit sec8 binds to postsynaptic density protein-95 (PSD-95): a novel interaction regulated by cypin (cytosolic PSD-95 interactor). *Biochem. J.* **2003**, *373* (Pt 1), 49–55.
- (89) Firestein, B. L.; Firestein, B. L.; Brenman, J. E.; Aoki, C.; Sanchez-Perez, A. M.; El-Husseini, A. E.; Bredt, D. S. Cypin: a cytosolic regulator of PSD-95 postsynaptic targeting. *Neuron* **1999**, *24* (3), 659–72.
- (90) Doran, J. F.; Jackson, P.; Kynoch, P. A.; Thompson, R. J. Isolation of PGP 9.5, a new human neurone-specific protein detected by high-resolution two-dimensional electrophoresis. *J. Neurochem.* **1983**, *40* (6), 1542–7.
- (91) Ardley, H. C.; Scott, G. B.; Rose, S. A.; Tan, N. G.; Robinson, P. A. UCH-L1 aggresome formation in response to proteasome impairment indicates a role in inclusion formation in Parkinson's disease. *J. Neurochem.* **2004**, *90* (2), 379–91.
- (92) Lowe, J.; McDermott, H.; Landon, M.; Mayer, R. J.; Wilkinson, K. D. Ubiquitin carboxyl-terminal hydrolase (PGP 9.5) is selectively present in ubiquitinated inclusion bodies characteristic of human neurodegenerative diseases. *J. Pathol.* **1990**, *161* (2), 153–60.
- (93) Eom, C. Y.; Heo, W. D.; Craske, M. L.; Meyer, T.; Lehman, I. R. The neural F-box protein NFB42 mediates the nuclear export of the herpes simplex virus type 1 replication initiator protein (UL9 protein) after viral infection. *Proc. Natl. Acad. Sci. U.S.A.* **2004**, *101* (12), 4036–40.
- (94) Bai, C.; Sen, P.; Hofmann, K.; Ma, L.; Goebel, M.; Harper, J. W.; Elledge, S. J. SKP1 connects cell cycle regulators to the ubiquitin proteolysis machinery through a novel motif, the F-box. *Cell* **1996**, *86* (2), 263–74.
- (95) Erhardt, J. A.; Hynicka, W.; DiBenedetto, A.; Shen, N.; Stone, N.; Paulson, H.; Pittman, R. N. A novel F box protein, NFB42, is highly enriched in neurons and induces growth arrest. *J. Biol. Chem.* **1998**, *273* (52), 35222–7.
- (96) Dagda, R. K.; Zhu, J.; Kulich, S. M.; Chu, C. T. Mitochondrially localized ERK2 regulates mitophagy and autophagic cell stress: implications for Parkinson's disease. *Autophagy* **2008**, *4* (6), 770–82.
- (97) Schmitt, O.; Eggers, R.; Haug, H. Topologic distribution of different types of neurons in the human putamen. *Anal. Quant. Cytol. Histol.* **2000**, *22* (2), 155–67.
- (98) Zhang, J.; Goodlett, D. R. Proteomic approach to studying Parkinson's disease. *Mol. Neurobiol.* **2004**, *29* (3), 271–88.
- (99) Fountoulakis, M.; Schuller, E.; Hardmeier, R.; Berndt, P.; Lubec, G. Rat brain proteins: two-dimensional protein database and variations in the expression level. *Electrophoresis* **1999**, *20* (18), 3572–9.
- (100) Larbi, N. B.; Jefferies, C. 2D-DIGE: comparative proteomics of cellular signalling pathways. *Methods Mol. Biol.* **2009**, *517*, 105–32.
- (101) Pietrogrande, M. C.; Marchetti, N.; Dondi, F.; Righetti, P. G. Decoding 2D-PAGE complex maps: relevance to proteomics. *J. Chromatogr., B: Analyt. Technol. Biomed. Life Sci.* **2006**, *833* (1), 51–62.
- (102) Zhang, X.; Fang, A.; Riley, C. P.; Wang, M.; Regnier, F. E.; Buck, C. Multi-dimensional liquid chromatography in proteomics—a review. *Anal. Chim. Acta (n/a)*, *664* (2), 101–13.
- (103) Basso, M.; Giraudo, S.; Corpillo, D.; Bergamasco, B.; Lopiano, L.; Fasano, M. Proteome analysis of human substantia nigra in Parkinson's disease. *Proteomics* **2004**, *4* (12), 3943–52.
- (104) Miyazaki, I.; Asanuma, M. Approaches to prevent dopamine quinone-induced neurotoxicity. *Neurochem. Res.* **2009**, *34* (4), 698–706.
- (105) Van Laar, V. S.; Dukes, A. A.; Cascio, M.; Hastings, T. G. Proteomic analysis of rat brain mitochondria following exposure to dopamine quinone: implications for Parkinson disease. *Neurobiol. Dis.* **2008**, *29* (3), 477–89.
- (106) Kaariainen, T. M.; Pilttonen, M.; Ossola, B.; Kekki, H.; Lehtonen, S.; Nenonen, T.; Lecklin, A.; Raasmaja, A.; Mannisto, P. T. Lack of robust protective effect of quercetin in two types of 6-hydroxydopamine-induced parkinsonian models in rats and dopaminergic cell cultures. *Brain Res.* **2008**, *1203*, 149–59.
- (107) Jin, J.; Meredith, G. E.; Chen, L.; Zhou, Y.; Xu, J.; Shie, F. S.; Lockhart, P.; Zhang, J. Quantitative proteomic analysis of mitochondrial proteins: relevance to Lewy body formation and Parkinson's disease. *Brain Res. Mol. Brain Res.* **2005**, *134* (1), 119–38.
- (108) Xun, Z.; Sowell, R. A.; Kaufman, T. C.; Clemmer, D. E. Protein expression in a Drosophila model of Parkinson's disease. *J. Proteome Res.* **2007**, *6* (1), 348–57.
- (109) Ichibangase, T.; Saimaru, H.; Takamura, N.; Kuwahara, T.; Koyama, A.; Iwatsubo, T.; Imai, K. Proteomics of Caenorhabditis elegans over-expressing human alpha-synuclein analyzed by fluorogenic derivatization-liquid chromatography/tandem mass spectrometry: identification of actin and several ribosomal proteins as negative markers at early Parkinson's disease stages. *Biomed. Chromatogr.* **2008**, *22* (3), 232–4.
- (110) Rodriguez, M.; Abdala, P.; Obeso, J. A. Excitatory responses in the 'direct' striatonigral pathway: effect of nigrostriatal lesion. *Mov. Disord.* **2000**, *15* (5), 795–803.
- (111) Smith, A. D.; Amalric, M.; Koob, G. F.; Zigmond, M. J. Effect of bilateral 6-hydroxydopamine lesions of the medial forebrain bundle on reaction time. *Neuropsychopharmacology* **2002**, *26* (6), 756–64.
- (112) Gonzalez-Hernandez, T.; Barroso-Chinea, P.; Rodriguez, M. Response of the GABAergic and dopaminergic mesostriatal projections to the lesion of the contralateral dopaminergic mesostriatal pathway in the rat. *Mov. Disord.* **2004**, *19* (9), 1029–1042.
- (113) Soderstrom, K. E.; O'Malley, J. A.; Levine, N. D.; Sortwell, C. E.; Collier, T. J.; Steece-Collier, K. Impact of dendritic spine preservation in medium spiny neurons on dopamine graft efficacy and the expression of dyskinesias in parkinsonian rats. *Eur. J. Neurosci.*
- (114) Esposito, A.; Dohm, C. P.; Kermer, P.; Bahr, M.; Wouters, F. S. alpha-Synuclein and its disease-related mutants interact differentially with the microtubule protein tau and associate with the actin cytoskeleton. *Neurobiol. Dis.* **2007**, *26* (3), 521–31.
- (115) Leverenz, J. B.; Umar, I.; Wang, Q.; Montine, T. J.; McMillan, P. J.; Tsuang, D. W.; Jin, J.; Pan, C.; Shin, J.; Zhu, D.; Zhang, J. Proteomic identification of novel proteins in cortical lewy bodies. *Brain Pathol.* **2007**, *17* (2), 139–45.
- (116) Hong, Z.; Zhang, Q. Y.; Liu, J.; Wang, Z. Q.; Zhang, Y.; Xiao, Q.; Lu, J.; Zhou, H. Y.; Chen, S. D. Phosphoproteome study reveals Hsp27 as a novel signaling molecule involved in GDNF-induced neurite outgrowth. *J. Proteome Res.* **2009**, *8* (6), 2768–87.
- (117) Zhou, Y.; Wang, Y.; Kovacs, M.; Jin, J.; Zhang, J. Microglial activation induced by neurodegeneration: a proteomic analysis. *Mol. Cell. Proteomics* **2005**, *4* (10), 1471–9.
- (118) Periquet, M.; Corti, O.; Jacquier, S.; Brice, A. Proteomic analysis of parkin knockout mice: alterations in energy metabolism, protein handling and synaptic function. *J. Neurochem.* **2005**, *95* (5), 1259–76.
- (119) Wooten, G. F.; Collins, R. C. Metabolic effects of unilateral lesion of the substantia nigra. *J. Neurosci.* **1981**, *1* (3), 285–91.
- (120) Zhang, W.; Wang, T.; Pei, Z.; Miller, D. S.; Wu, X.; Block, M. L.; Wilson, B.; Zhang, W.; Zhou, Y.; Hong, J. S.; Zhang, J. Aggregated alpha-synuclein activates microglia: a process leading to disease progression in Parkinson's disease. *FASEB J.* **2005**, *19* (6), 533–42.
- (121) Reynolds, A. D.; Glanzer, J. G.; Kadiu, I.; Ricardo-Dukelow, M.; Chaudhuri, A.; Ciborowski, P.; Cerny, R.; Gelman, B.; Thomas, M. P.; Mosley, R. L.; Gendelman, H. E. Nitrated alpha-synuclein-activated microglial profiling for Parkinson's disease. *J. Neurochem.* **2008**, *104* (6), 1504–25.
- (122) Beal, M. F. Mitochondria, oxidative damage, and inflammation in Parkinson's disease. *Ann. N.Y. Acad. Sci.* **2003**, *991*, 120–31.
- (123) Hald, A.; Lotharius, J. Oxidative stress and inflammation in Parkinson's disease: is there a causal link. *Exp. Neurol.* **2005**, *193* (2), 279–90.
- (124) Rogers, J.; Mastroeni, D.; Leonard, B.; Joyce, J.; Grover, A. Neuroinflammation in Alzheimer's disease and Parkinson's

- disease: are microglia pathogenic in either disorder. *Int. Rev. Neurobiol.* **2007**, *82*, 235–46.
- (125) Hald, A.; Van Beek, J.; Lotharius, J. Inflammation in Parkinson's disease: causative or epiphenomenal. *Subcell Biochem.* **2007**, *42*, 249–79.
- (126) Rojo, A. I.; Innamorato, N. G.; Martin-Moreno, A. M.; De Ceballos, M. L.; Yamamoto, M.; Cuadrado, A. Nrf2 regulates microglial dynamics and neuroinflammation in experimental Parkinson's disease. *Glia* 2009.
- (127) Ghorayeb, I.; Puschban, Z.; Fernagut, P. O.; Scherfler, C.; Rouland, R.; Wenning, G. K.; Tison, F. Simultaneous intrastriatal 6-hydroxydopamine and quinolinic acid injection: a model of early-stage striatonigral degeneration. *Exp. Neurol.* **2001**, *167* (1), 133–47.

PR100389U